공학박사 학위논문

Simple and Economic Methods to Improve Li-S Battery Performance

리튬-황 전지의 성능향상을 위한 간단하고 경제적인 방법

2016년 8월

서울대학교 대학원
화학생물공학부
김 귀 룡

Abstract

Simple and Economic Methods to Improve Li-S Battery Performance

Kwi Ryong Kim

School of Chemical & Biological Engineering

Seoul National University

Lithium ion batteries (LIBs) have been widely used as main power sources for portable electronic devices such as cellular phones and laptop computers. However, the energy density of LIBs can't satisfy the continuous demand for increased energy density requirement, especially for electric vehicles (EVs) and energy storage systems (ESSs). One of the most promising candidates for next generation batteries is the lithium-sulfur (Li-S) battery, which has theoretical specific capacity of 1672 mAh g^{-1}. However, there are still many obstacles for its practical application. First, the sulfur has extremely low electrical and ionic conductivities. It leads to limited sulfur utilization for electrochemical reaction. And a large amount of conductive agent is normally used to compensate the limited conductivities, ultimately the sulfur content in cathode is very low. Second, the poor cycle performance. There are many factors responsible for cycle fading. The main two factors are the soluble reaction intermediates (polysulfides) and the volume change during charge/discharge processes. The dissolution of polysulfides leads to continuous active material loss from cathode, and the volume change can induce the increase of cathode impedance from the structure collapse.

Many approaches for advancing Li-S batteries have been reported during past few decades. One of the most effective and popular methods of overcoming the problems mentioned above is based on the infiltration of sulfur into carbonaceous materials with high specific surface area and large pore volumes. The high surface area not only increases the electronic contact area between carbon and sulfur, but also provides more reaction sites. Furthermore, the pores in carbonaceous materials can physically trap dissolved polysulfides and accommodate the volume change during cycling, which is beneficial for maintaining electronically conductive networks. Another method is introducing conductive and sulfiphilic surface (e.g., functionalized carbon, metal oxide, metal sulfide or metal carbide) that effectively adsorbs sulfur species. However, there are little researches on practically available methods. In this dissertation, I will introduce two economic and simple methods for advancing Li-S batteries.

In first part of chapter 1, I generally discuss LIBs. An overview of basic knowledge of batteries and materials currently being used for the cathode and anode of LIBs are introduced. In addition, a general introduction about Li-S batteries is followed. I also briefly summarized recent issues on Li-S batteries.

In chapter 2, I introduce a powerful and economical method through a very simple electrochemical control to improve the cycle life performance. Several discharge and charge cycles at high-potential regions (i.e., above 2.2 V vs. Li/Li^+) before cycling result in the dissolution of a certain amount of polysulfide into the electrolyte, as well as the redistribution of sulfur on the cathode. Ultimately, these processes significantly enhance the cycle retention of Li-S battery. This approach is based on an electrochemical technique refer to as “activation-cycling”. It is not only very simple but also can apply to all kinds of sulfur cathodes. In particular, cycling stability of bare sulfur cathode, which normally is considered to be poor and difficult to be improved without materials modifications, can be simply enhanced by activation cycling. I

analyze the effects of this process in terms of dissolved polysulfides, and sulfur redistribution in cathode structure by the electrochemical impedance spectroscopy (EIS) and scanning photoelectron microscopy (SPEM) analysis.

In chapter 3, I will report on the use of a redox mediator as an electron-hole transfer agent between the solid electrode and polysulfides in the electrolyte. This novel approach successfully realized the high performance Li-S battery for ultra-high sulfur content (80 wt%) cathode. The effective cathode conductivity is increased by introducing a redox mediator (cobaltocene) into the electrolyte. It has a redox potential within the region of polysulfide reduction. I confirmed that cobaltocene enabled Li_2S nucleation and growth not only on the conductive carbon surface but also in the electrolyte. The redox mediator acts as an electron transfer agent: it is reduced at the cathode and then oxidized by the polysulfides remote from the conductive surface to produce Li_2S. Taken together, this unified mechanism allows sufficient Li_2S formation with a very low amount of conductive agent in the cathode. It is confirmed by electrochemical method, scanning electron microscope (SEM), X-ray absorption near edge structure (XANES) and in-situ XRD studies.

***Keywords*:** Lithium-sulfur battery, electrochemical method, redistribution of sulfur, redox mediator, cobaltocene, ultra-high sulfur content, economic and simple methods

***Student Number*:** 2011-22914

Contents

List of Tables

List of Figures

Chapter 1. Introduction

1.1. General introduction of batteries

Lithium ion batteries (LIBs) are widely used as energy storage devices for portable electronics in the past few decades due to relatively high energy density compare to other energy storage systems (Figure 1.1) [1]. Batteries are devices that provide electrical power from a chemical energy source. The energy source contains two reactive materials that are capable of a spontaneous oxidation-reduction reaction. The free energy of this chemical reaction is converted into electrical energy. The equilibrium potential E_0 of a cell reaction is related to the change in Gibbs energy by Faraday constant (F) and the number of electrons that are transferred (n).

$E_0 = -\Delta G/nF$

Some batteries may be recharged and used many times, whereas other batteries can only be discharged one time. If a battery is designed to be discharged only once, it is called a 'primary battery'. Rechargeable batteries can be discharged and then recharged to their original fully charged condition by reversing the current flow, it is called a 'secondary battery'.

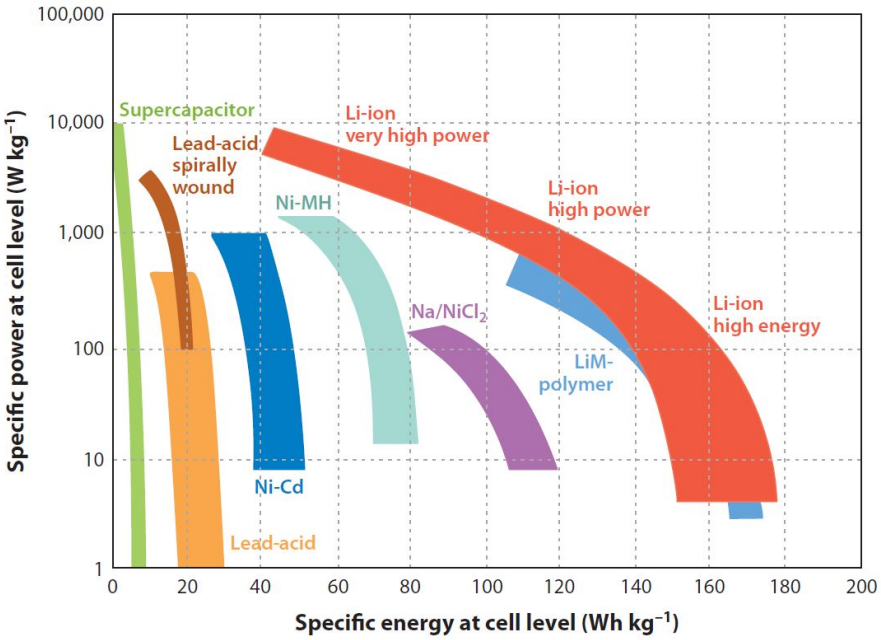

Figure 1.1 A comparison of the energy and power densities of common rechargeable batteries. Adapted from Ref [1] (C. M. Hayner, X. Zhao and H. H. Kung, *Annu. Rev. Chem. Biomol. Eng.*, 2012, 3, 445).

The fundamental unit of a secondary battery is an electrochemical cell, which consists of a negative electrode and a positive electrode usually separated by a porous polymer material impregnated with an ionic conductor called an electrolyte (Figure 1.2) [2]. This prevents the anode from contacting the cathode and shorting the cell. The electrons produced by the electrochemical oxidation, $A \rightarrow A^{x+} + xe^-$, during discharge at the negative electrode (anode) flow into the external circuit where they perform useful work and then enter the positive electrode through the electrochemical reduction, $C + xe^- \rightarrow C^{x-}$, at the cathode. An electrochemical cell is a reactor for such controlled redox reactions, and the electronic barrier separating positive and negative electrodes is called 'electrolyte'. The electrolyte exists ubiquitously in all electrochemical devices. For the electrochemical reactor to operate sustainably, the electrolyte has to be ionically conductive in addition to being electronically insulating, so that mass transport of charge carriers through it can proceed to offset the charge separation incurred by the orientation movement of electrons. As most electrolytes are in liquid state, consisting of an ionic compound (salt) dissolved in liquid solvent, a physical battier, typically a polyolefin film that has interconnecting porosity and can be soaked in electrolyte solution, is usually required as the mechanical support to

achieve the physical separation of electrodes. As fundamental qualifications, an electrolyte should be stable against both the oxidative decompositions at the positive surface and reductive decompositions at the negative surface.

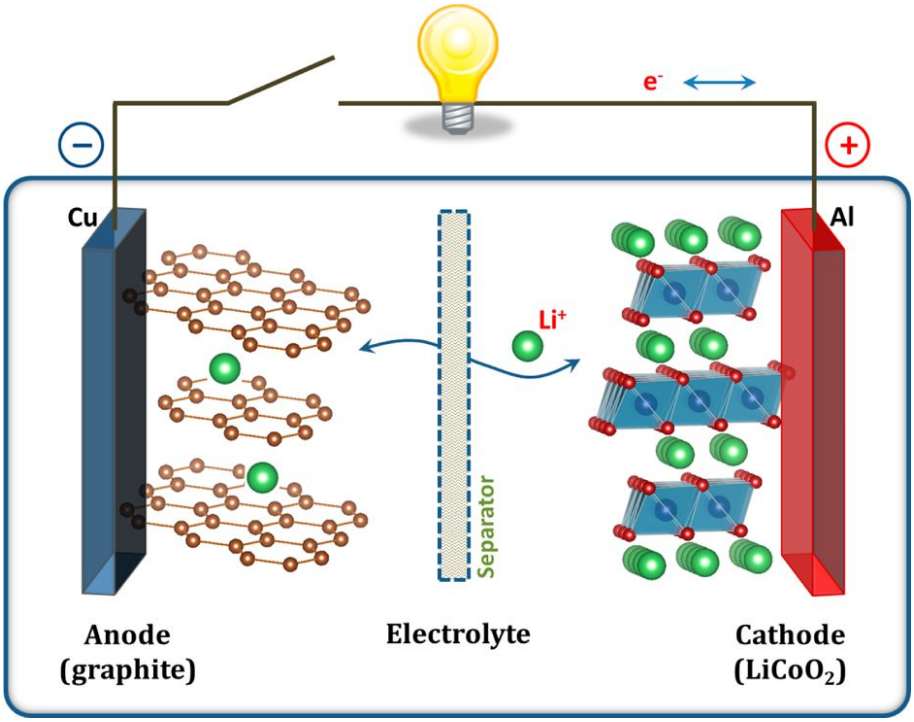

Fig. 1.2 Schematic illustration of the lithium ion battery. Adapted from Ref [2] (J. B. Goodenough and K. -S. Park, *J. Am. Chem. Soc*., 2013, 135, 1167).

1.2. General introduction of Li-ion batteries

1.2.1. Anode materials for Li-ion batteries

The commercially used anode material is graphite, which is working through intercalation mechanism [3]. A low discharge potential and high capacities per unit mass and volume are essential for negative electrodes in batteries. From these viewpoints, lithium metal is the most attractive material as a negative electrode because it has an extremely low redox potential (-3.045 V vs. standard hydrogen electrode) and high gravimetric and volumetric capacities (3860 mAh g^{-1} and 2062 mAh cm^{-3}, respectively). In fact, lithium metal has been used as a negative electrode in primary lithium batteries since the 1980s. However, it has not been used in rechargeable lithium batteries, because of its poor cyclability and safety in repeated charge/discharge cycles. Lithium metal deposited in nonaqueous electrolytes sometimes exhibits a dendrite shape (Figure 1.3) [4]. In general, this dendrite of lithium is so active that an explosion of secondary lithium batteries may occasionally occur. Instead of lithium metal, carbonaceous materials, typically graphite, have been used as negative electrodes in rechargeable lithium cells. Lithium ions can be reversibly intercalated within carbonaceous materials upon charging and

deintercalate

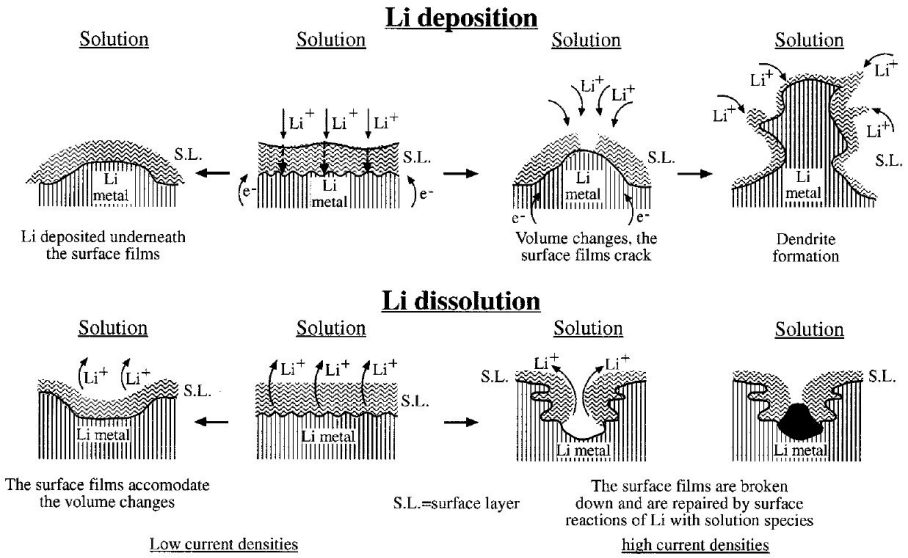

Figure 1.3. An illustration of the morphological phenomena developed on Li electrodes during Li deposition and dissolution. Adapted from Ref [4] (Y. S. Cohen, Y. Cohen and D. Aurbach, *J. Phys. Chem. B*, 2000, **104**, 12282.).

upon discharging as follows.

$$C + xLi^+ + xe^- \leftrightarrow Li_xC$$

Graphite is a typical layered compound that consists of hexagonal sheets of sp2-carbon atoms (called graphene sheets), weakly bonded together by van der Waals forces into an ABAB… stacking sequence along the c-axis. Graphite can intercalate up to one Li atom per six C atoms under ambient conditions, a specific capacity of 372 mAh g^{-1} results (Figure 1.4) [5].

A further increase of cell energy strongly depends on the development of new electrode materials with higher charge density. As negative electrode materials, the advantage of lithium alloys (Figure 1.5) [6] and conversion materials (Figure 1.6) [7] over graphite in energy density, especially volumetric energy density, is evident. Therefore, intensive research about alloying and conversion anode materials are being done. The anode materials that undergo alloying reaction with lithium generally deliver high gravimetric and volumetric capacities. However, as a trade-off to high specific capacities, these alloying materials suffer from extreme volume expansion and contraction during lithiation and de-lithiation, which causes cracks and pulverization of active materials, which eventually leads to capacity fading. Many methods such as morphology control and nanocomposites with carbon

have been introduced to overcome this problem [8-10]. Conversion reactions are lithium reactions with binary M-X compounds (M=transition metal and X=O, N, F, S, P) in which M-X compound is fully reduced to nanoscale metal clusters (3-5 nm) dispersed in a Li_nX matrix as follows.

$$\text{nano-}M_aX_b + (b \bullet n)Li \leftrightarrow \text{nano-}aM + bLi_nX$$

where n is formal oxidation state of X (Figure 1.7) [11].

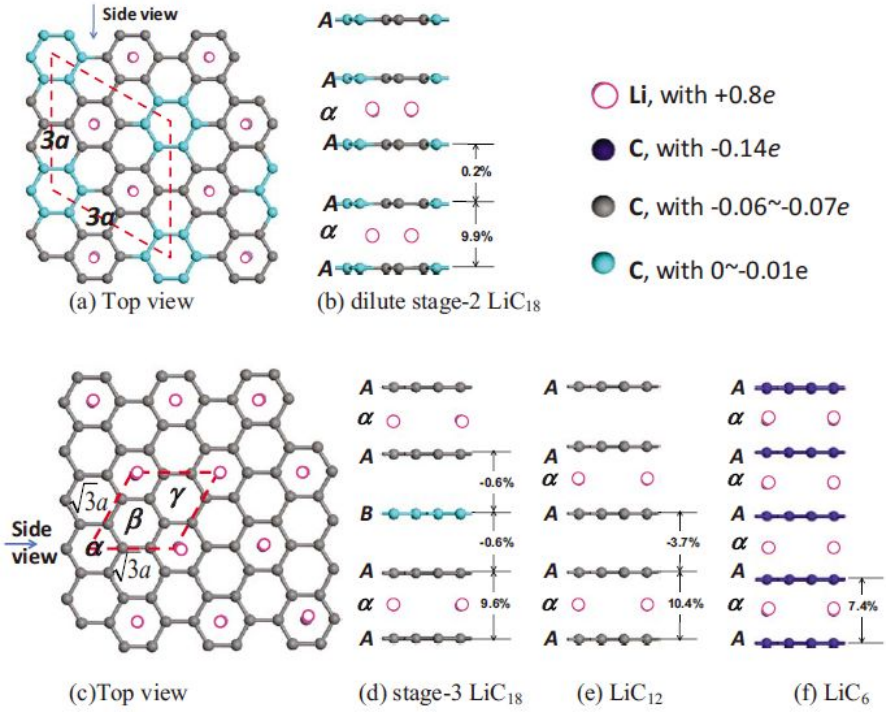

Figure 1.4. Atomic structure of Li-intercalated compounds of graphite. Adapted from Ref [5] (Y. Qi, H. Guo, L. G. Hector and A. Timmons, *J. Electrochem. Soc.*, 2010, **157**, A558.).

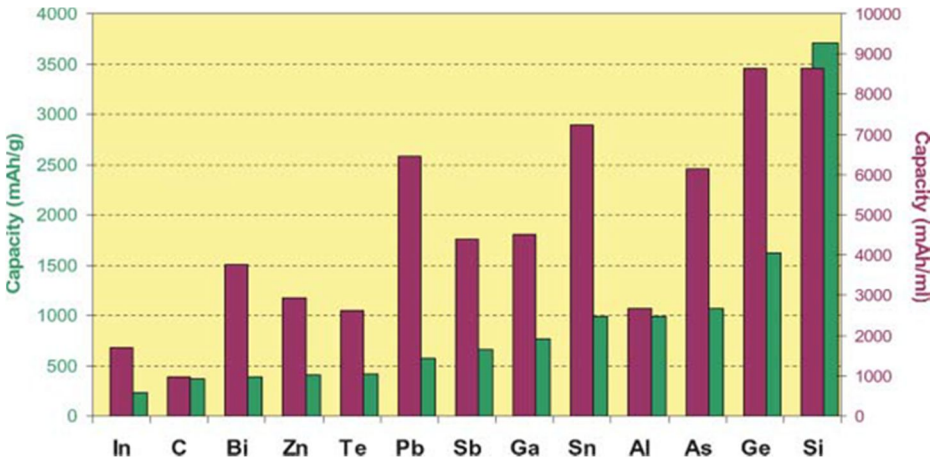

Figure 1.5. Gravimetric and volumetric capacities for selected alloying reactions. Capacities for graphite are given as references. Adapted from Ref [6] (D. Larcher, S. Beattie, M. Morcrette, K. Edstrom, J. -C. Jumas and J. -M. Tarascon, *J. Mater. Chem*., 2007, **17**, 3759).

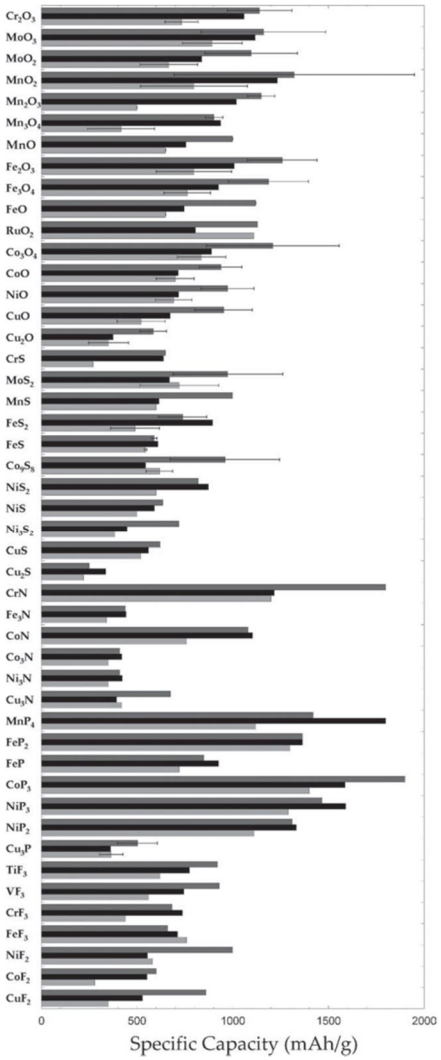

Figure 1.6. Theoretical (black bars), first discharge (dark grey) and charge (light grey) specific capacities of different compounds that react with lithium through a conversion reaction. Adapted from Ref [7] (J. Cabana, L. Monconduit, D. Larcher and M. R. Palacin, *Adv. Mater.*, 2010, **22**, E170).

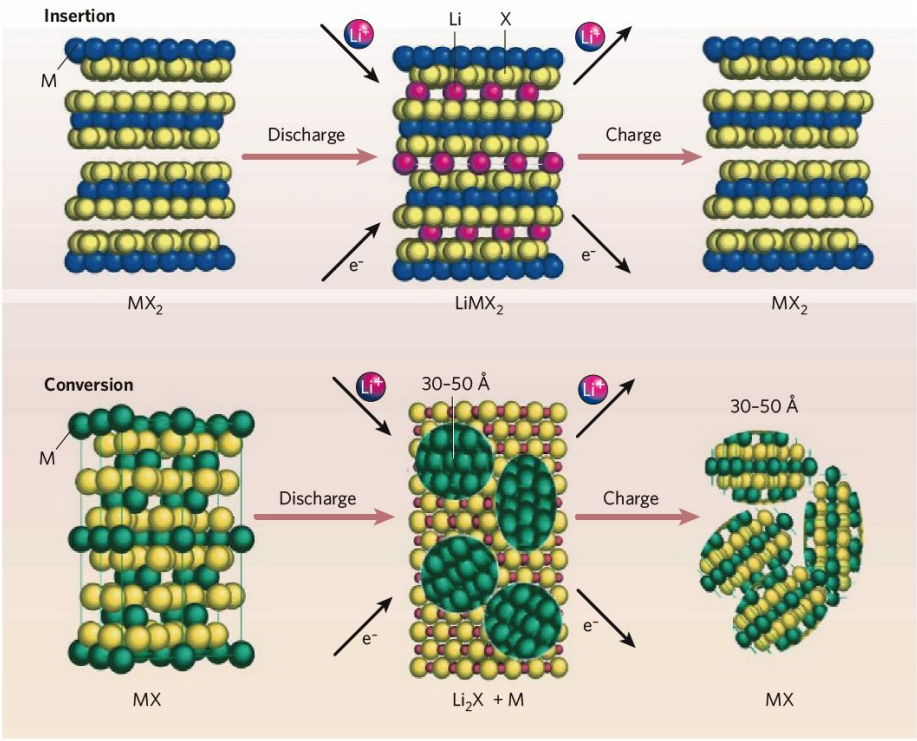

Figure 1.7. Schematic representation showing the contrasting reaction mechanisms occurring during discharge for insertion (top) and conversion reactions (bottom). The insertion reaction demonstrates a maximum of 1 electron transfer per transition metal (here designated M), whereas the conversion reaction can transfer 2 to 6 electrons. Adapted from Ref [11] (M. Armand and J.-M. Tarascon, *Nature*, 2008, **451**, 652.).

1.2.2. Cathode materials for Li-ion batteries

In the other hand, intercalation mechanism based crystal materials are used as cathode materials. The most commonly used material is layered oxide material ($LiCoO_2$). An insertion compound is a host solid into/from which a guest atom can be reversibly inserted/extracted in a topotactic reaction, that is, with only displacive changes of the atomic positions of the host. In the early 1970s, it was suggested and later demonstrated that titanium disulfide (TiS_2) is a lithium-insertion compound that can be used as a cathodic host for a lithium rechargeable battery [12]. The sulfur atoms of titanium disulfide have a hexagonal close-packed structure with titanium located in alternate basal planes of octahedral sites. The strongly bound edge-shared octahedral sites form titanium disulfide layers that are held together by weak van der Waals bonding, and lithium can be inserted reversibly into the empty planes of octahedral sites of the wan der Waals gap. In the electrochemical reaction at the cathode, electrons from the external circuit reduce Ti^{4+} to Ti^{3+} and the Li^+ ions enter the host from the electrolyte to balance the charge in the reaction as follows.

$$TiS_2 + xLi^+ + xe^- \leftrightarrow Li_xTiS_2$$

As illustrated in Figure 1.8 [13]. However, TiS_2 has low redox potential

respectively. The sulfide cannot take advantage of the large voltage window

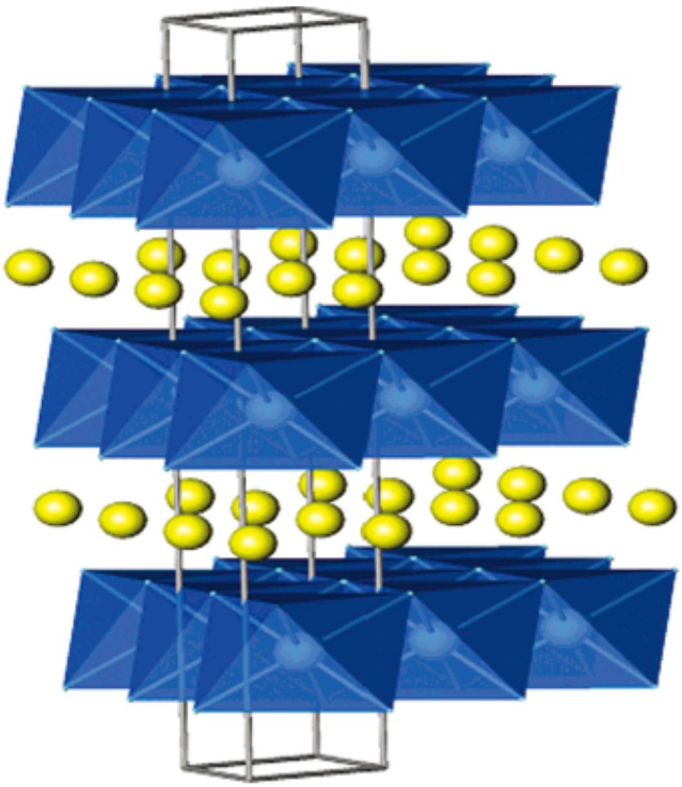

Figure 1.8. Layered structure of $LiTiS_2$. Adapted from Ref [13] (M. S. Whittingham, *Chem. Rev.*, 2004, **104**, 4271.)

offered by the nonaqueous electrolytes. On the contrary, higher oxidation states can be realized in first-row transition metal oxides. Therefore, oxide-insertion compounds are used as cathodes in rechargeable lithium batteries.

Lithium cobalt oxide is the first reported and best-known compound to exhibit a high voltage of over 4 V with respect to a lithium negative electrode. $LiCoO_2$ has the α-$NaFeO_2$ structure with the oxygens in a cubic close-packed arrangement (Figure 1.9a) [14]. The complete removal of lithium from $LiCoO_2$ occur oxygen layers rearrange themselves to give hexagonal close packing of the oxygen. Ultimately, the producing of cobalt dioxide (CoO_2) corresponds to a theoretical specific capacity of 274 mAh g^{-1}. However, the over delithiation can induce phase transition and results in noticeable capacity fading. The chemical composition range, in which reversible lithium extraction/insertion is ensured, is generally limited to $0.5 \leq x \leq 1.0$ in Li_xCoO_2. This corresponds to a specific capacity of 137 mAh g^{-1} and a Li/Li_xCoO_2 battery operating voltage range of 3.0-4.2 V [15].

There are also spinel and olivine oxide structure cathode materials. The most well-known spinel oxide is $LiMn_2O_4$, and olivine oxide is $LiFePO_4$ (Figure 1.9b and c). $LiMn_2O_4$ shows many advantages as cathode materials including low cost, low toxic, good structural stability of Mn^{3+}/Mn^{4+} redox

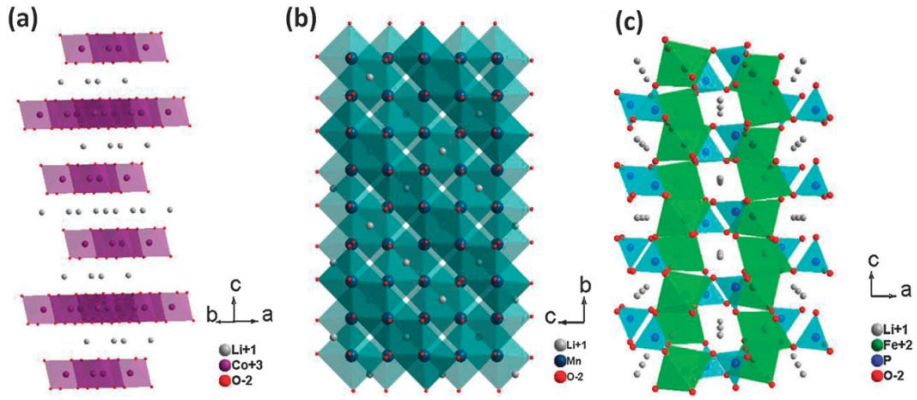

Fig. 1.9. Schematic crystal structures of three types of cathode materials: (a) $LiCoO_2$, (b) $LiMn_2O_4$ and (c) $LiFePO_4$. Adapted from Ref [14] (H. Wang and H. Dai, *Chem. Soc. Rev.*, 2013, **42**, 3088).

couple, high power capability due to 3D framework. The theoretical capacity of $LiMn_2O_4$ is 148 mAh g^{-1}, but the practical capacity of around 120 mAh g^{-1} is obtained. The main problem with using $LiMn_2O_4$ as a cathode is cycle fading, which is related to dissolution of manganese into the electrolyte and phase transition [16]. Olivine $LiFePO_4$ is the one of the most attractive cathodes among polyanion oxides because of its low cost, low toxic, environment friendliness, high cyclic stability and high thermal stability. $LiFePO_4$ has a reasonable high theoretical capacity of 170 mAh g^{-1} and a high practical capacity of around 165 mAh g^{-1}. The main drawbacks are low energy density associated with the low reaction voltage of Fe^{3+}/Fe^{2+} and low rate capability due to 1D ionic channel and poor electron conductivity [17-19].

1.3. General introduction of Li-S batteries

Rechargeable lithium batteries have gained a commendable position in the field of advanced power sources and have replaced many other batteries in the market, particularly in the areas of portable electronic devices and power tools. The state-of-the-art lithium-ion batteries perform satisfactorily for many applications with a practical specific energy of about 150 Wh kg^{-1}. However, there is an ever-increasing demand for the development of suitable secondary batteries that provide higher specific energies for various applications such as in electric vehicles (Figure 1.10) [20] and energy storage systems.

The Lithium-sulfur (Li-S) battery is considered as very promising candidate for next generation batteries. By combining lithium metal and elemental sulfur with theoretical specific capacities of 3830 and 1672 mAh g^{-1}, respectively. Since sulfur is a relatively cheap and abundantly available material, the cost of the Li-S battery is much lower when compared to other batteries [21-24].

The possibility of using the Li-S cell was reported in the early 1970s. However, the development of rechargeable Li-S cells passed through a number of technologically demanding phases. Several bottlenecks, such as the insulating nature of sulfur, the solubility of internal discharge products in the

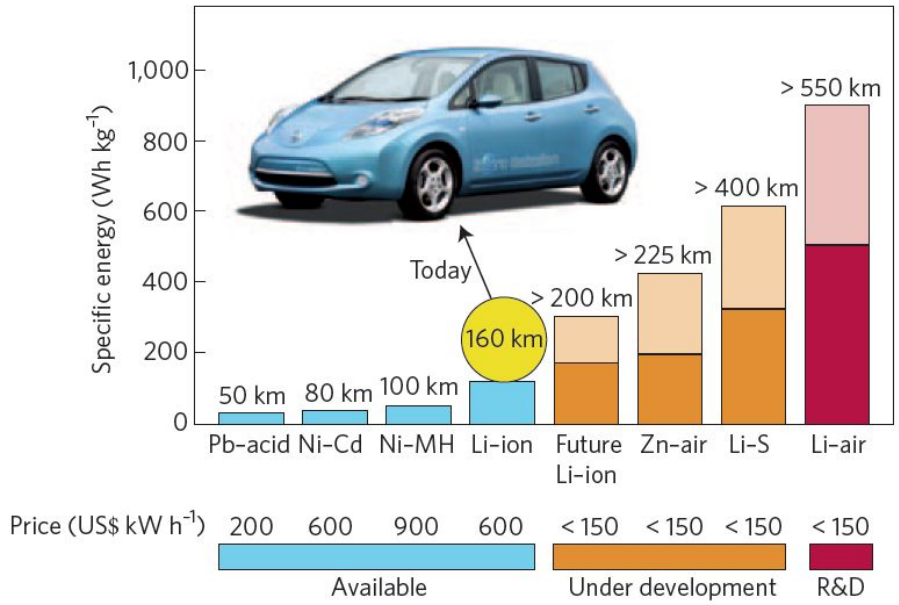

Figure 1.10. Practical specific energies for some rechargeable batteries, along with estimated driving distances and pack prices. Adapted from Ref [20] (P. G. Bruce, S. A. Freunberger, L. J. Hardwick and J. M. Tarascon, *Nat. Mater.*, 2012, **11**, 19.)

electrolytes, and poor cycle property, had to be overcome. Early research concentrated on using sulfur in the vapor or molten state as electrode material together with molten polysulfides and solid electrolytes. Rechargeable, ambient-temperature Li-S batteries were not considered commercially viable until the mid-1990s when a few patents were filed, which demonstrated high sulfur utilization and long cycle life. Following this, the studies on rechargeable Li-S cells gained momentum.

Li-S battery uses elemental sulfur as the cathode and lithium as the anode. The charge/discharge processes are schematically represented in Figure 1.11 [25]. At the open-circuit state, the Li-S battery holds a maximum voltage (Φ_{oc}), which is in direct proportion to the difference between the electrochemical potentials of the Li anode (μ_a) and the S cathode (μ_c). Upon discharging, S_8 reacts with Li by a multi-electron reduction process to form polysulfide intermediates (Li_2S_x, x=2-8), and to generate lithium sulfide (Li_2S) at the end of discharge. This process is accompanied by an increase in cathode electrochemical potential until the battery reaches the terminal voltage (normally$\leq$1.5 V). The reverse reaction occurs when an external electric field with a certain potential difference is applied, leading to the decomposition of Li_2S back to Li and S [26-29].

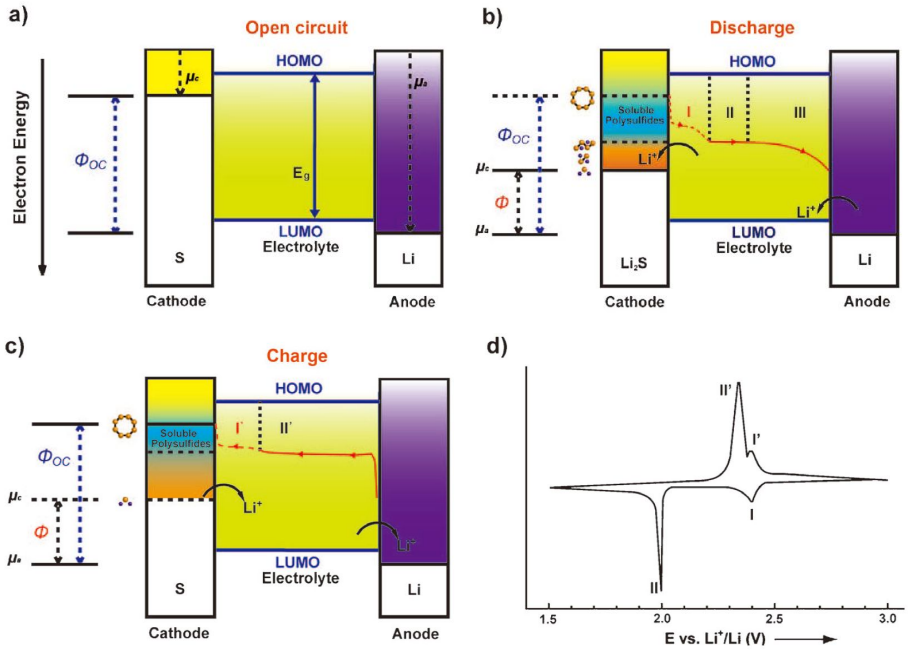

Figure 1.11. Electrochemistry of the Li-S battery at different stage: a) open circuit; b) discharge process; c) charge process. d) Typical cyclic voltammogram (CV) for an S cathode in a Li-S battery. Adapted from Ref [25] (Y. X. Yin, S. Xin, Y. G. Guo and L. J. Wan, *Angew. Chem. Int. Ed.*, 2013, **52**, 13186.)

As mentioned above, there are many problems that hinder the practical application of the Li-S battery. First, sulfur, the active material of battery, is electronic and ionic insulator, which increase the internal resistance of the battery. In order to compensate for the low electrical conductivity of sulfur, huge amount of conductive agent is typically needed. It finally limited the amount of active material in the cathode and lowered energy density. Furthermore, the sulfur utilization is still low in spite of high conductive agent content in cathode. The second problem lies in the electrochemical process of the Li-S battery. There are several of polysulfides formed during charge/discharge process. Each intermediate product has a defined stability and solubility that is a function of the medium (identity of solutes and solvent) in which it is formed. Any soluble sulfur based species can diffuse out of the electrode, through the separator, to the lithium negative electrode. During charging, or simply from direct chemical reaction with lithium, these soluble sulfur-containing species will be reduced and ultimately deposited as insoluble Li_2S or short chain polysulfides. The process by which this occurs is essentially a form of self-discharge and loss of active material. Migration of sulfide species has further effects as the highly reduced species, Li_2S and short chain polysulfides, react with the S_x^{2-} from the electrolyte to form lower order

polysulfides. On diffusing back to the positive electrode, these species are then re-oxidized into high order polysulfides. The resultant internal "redox shuttle" lowers both the available discharge capacity and the efficiency of recharging. The third problem is related to the volume variation of the S cathode upon cycling. In the case of different molar densities of α-S (15.46 cm^3 mol^{-1}) and Li_2S (27.71 cm^3 mol^{-1}), sulfur experiences a noticeable expansion of about 79% upon Li uptake, which makes active material pulverize and lose their electrical contacts with the conductive substrate or the current collector. As the fraction of "non-contact S" increases in the cathode material, significant capacity fade is observed during cycling.

The three problems mentioned above are considered as major obstacles to Li-S battery commercialization. Many researches have been done for overcome these problems during past few decades. One of the most effective and popular methods is based on the infiltration of sulfur into carbonaceous materials with high specific surface areas and large pore volumes (Figure 1.12) [30-35]. The high surface area not only increase the electronic contact area between carbon and sulfur, but also provides more reaction sites. Furthermore, the pores in carbonaceous materials can physically trap dissolved polysulfides and accommodate the volume change during cycling, which is beneficial for

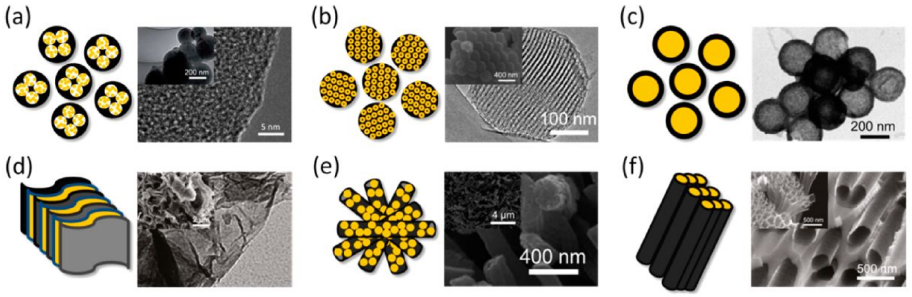

Figure 1.12. Hierarchical designs of carbon-based sulfur composites: (a) microporous carbon spheres, (b) spherical ordered mesoporous carbon nanoparticles, (c) porous hollow carbon, (d) graphene oxide sheets, (e) porous carbon nanofibers, and (f) hollow carbon nanofibers to encapsulate sulfur. Adapted from Ref [23] (A. Manthiram, Y. Fu, Y.-S. Su, *Acc. Chem. Res.*, 2013, **46**, 1125.)

maintaining electronically conductive networks. This kind of physical confinement can kinetically solve problems but still have many limitations. The pore volume of carbon can't be increased infinitely, since the increased pore volume achieved at the cost of reduced conductivity. Furthermore, the usually nonpolar C-C bonding can only provide polar polysulfide intermediates with a "sulfiphobic" surface [36,37]. Once polysulfides are solvated, they detach from the electrode surface as a result of poor affinity for the surface and diffuse away. Ultra-microporous carbon was employed to maximize the physical confinement. In this system, the electrolyte can't infiltrate into micropore and thus there isn't polysulfides formed during charge/discharge process. Instead, sulfur directly convert to Li_2S. Therefore, microporous carbon can effectively limit the dissolution out of polysulfides (Figure 1.13) [38,39]. However, due to limited pore volume and difficulties in sulfur infiltration, this method also sacrifices the sulfur content.

To address the issues of the poor interaction between polar sulfur species with cathode host, another promising approach is to adopt "sulfiphilic" surface chemistry (Figure 1.14) [40]. Some polar adsorbents, like metal oxide, metal sulfide, metal carbide and N- and/or S-doped carbon, have already been employed for use in sulfur cathodes [41-49]. Recent advances in modern

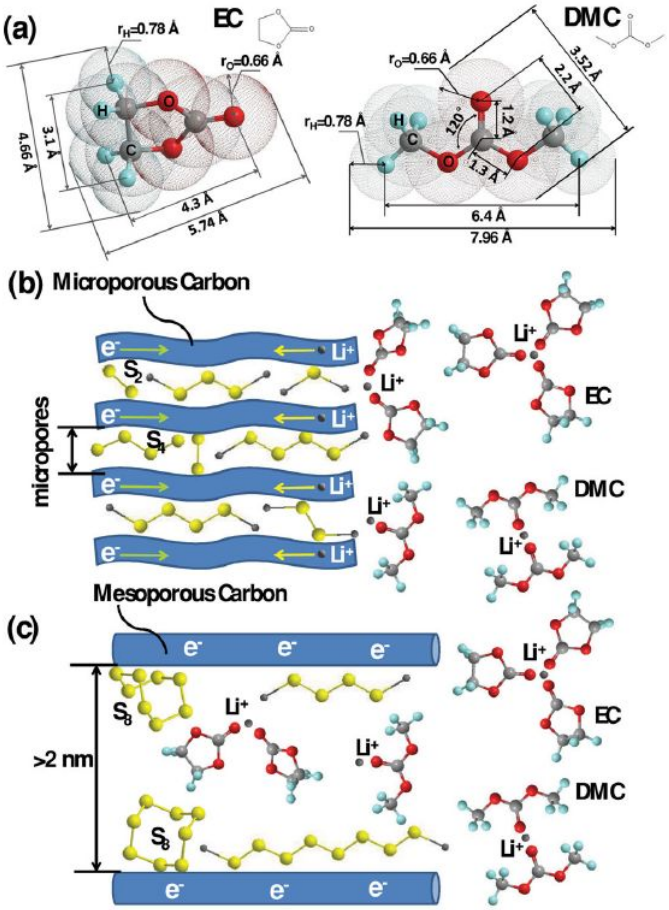

Figure 1.13. a) Theoretical calculation of the dimensions of EC and DMC molecules. Schematics of the lithiation process b) in a sulfur microporous carbon cathode and c) sulfur mesoporous carbon cathode in carbonate-based electrolyte. Adapted from Ref [39] (Z. Li, L. Yuan, Z. Yi, Y. Sun, Y. Liu, Y. Jiang, Y. Shen, Y. Xin, Z. Zhang, Y. Huang, *Adv. Energy Mater.*, 2014, **4**, 1301473.)

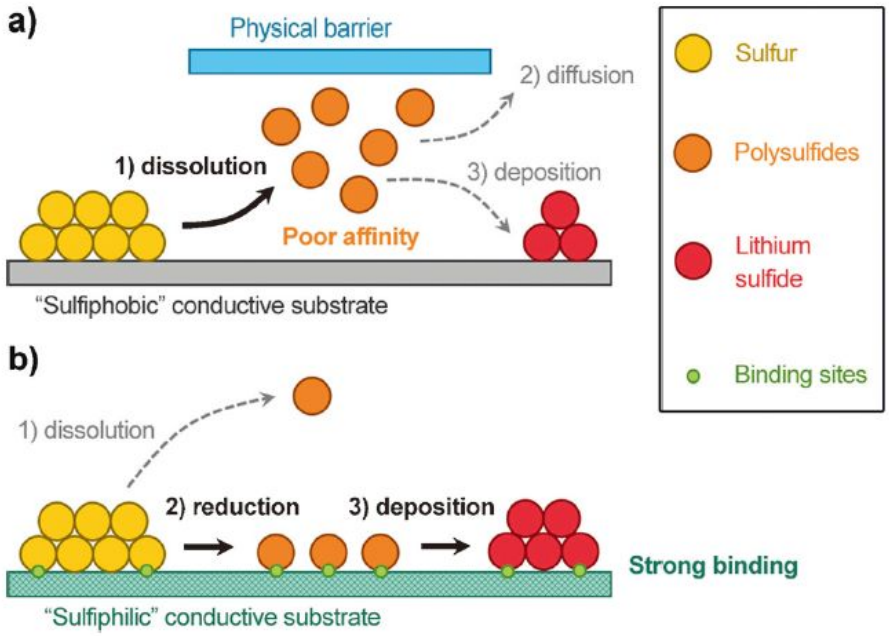

Figure 1.14. The two principles employed in the design of host materials for sulfur cathodes: a) Physical confinement of polysulfides by introducing an external barrier with a sulfiphobic conductive surface (for example, carbonaceous materials); and b) enhancing the affinity of the polysulfide intermediates for the surface by using polar adsorbents as sulfiphilic conductive substrates. Adapted from Ref [40] (H. J. Peng and Q. Zhang, *Angew. Chem. Int. Ed.*, 2015, 54, 11018.)

separators have also been demonstrated to affect the transport of polysulfides b etween the two electrodes [50].

More recently, it is reported that introducing a catalyst in the Li-S system to modify the electrode/electrolyte interface presents a new method for improving electrochemical performance. Some noble metals and transition metals can reduce overpotential and excellent specific capacity [51,52].

In order to replace the Li metal anode, Li_2S cathodes are also intensively researched [53]. The major problem of Li_2S cathode is the low utilization and large overpotential at first charging process. Many approaches, like carbon coating, introducing redox mediator and Li_2S solvating additives, have been reported as effective solutions [54-57].

1.4. Objectives of this dissertation

In this dissertation I tried to improve Li-S batteries electrochemical performance through economic and simple methods that commercially available.

Recent developed approaches for improving cycle stability of sulfur batteries such as infiltration of sulfur in porous carbon should involve time consuming and troublesome process, which hampers commercialization. At first part of this dissertation, I report on a novel method of improving the cycle life performance of lithium-sulfur batteries. This approach is based on an electrochemical technique refer to as "activation-cycling," which involves cycling at a low C-rate at the high plateau region (the polysulfides dissolution region) of the voltage curve before normal cycling. This strategy is not only very simple but also can apply to all kinds of sulfur cathodes. In particular, cycling stability of bare sulfur cathode, which normally is considered to be poor and difficult to be improved without materials modifications, can be simply enhanced by activation cycling. I analyze the effects of this process in terms of dissolved polysulfides, and explain how the capacity of sulfur cathode after 50 cycles can be doubled by adopting this technique. I confirmed that the sulfur was rearranged in cathode structure by

electrochemical method and scanning photoelectron microscopy analysis. I briefly summarized the research in Figure 1.15. I hope that this study will be helpful to further understand the fading mechanism of lithium sulfur batteries.

Due to the intense research on improving cycle stability of Li-S batteries, the cycle performance is dramatically enhanced during past few decades. However, the sulfur content in cathode is still very low (about 50 to 60 wt%), which hampers the commercialization. In the latter half of this dissertation, I report on a novel method for high electrochemical performance Li-S battery with ultra-high sulfur content (80 wt%) cathode using a redox mediator (cobaltocene). Cobaltocene is studied in the electrolyte of Li-S batteries for its role as an electron-hole transfer agent. Its redox reaction with polysulfides allows for effective electron transfer between the conductive surface of cathode and dissolved polysulfides. I schematically illustrated the working process of redox mediator in Figure 1.16. This improved conductivity enabled the construction of a cathode with ultra-high sulfur loading by reducing the need for conducting agent and binder. I demonstrated 200% increased capacity after 50 cycles and dramatically improved volumetric capacity, compared to the typical cathode. This result is relevant to researchers of electrochemistry, material science and power sources, and represents a crucial

innovation in developing Li-S batteries to replace the ubiquitous lithium-ion cells.

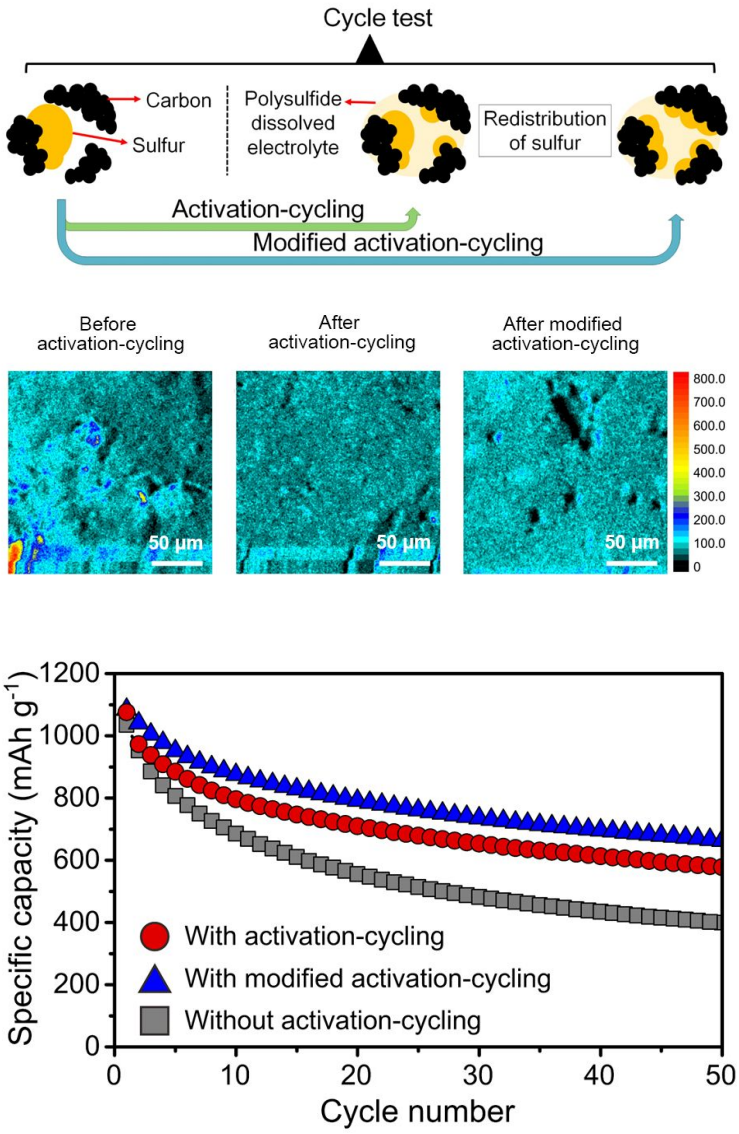

Figure 1.15. Briefly summarize the effect of activation-cycling process.

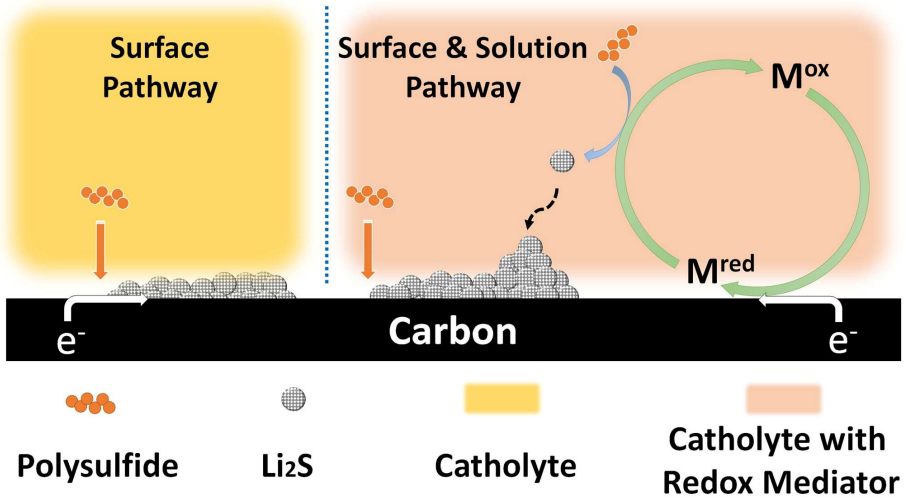

Figure 1.16. Schematically illustrated the working process of redox mediator.

1.5. References

[1] C. M. Hayner, X. Zhao and H. H. Kung, *Annu. Rev. Chem. Biomol. Eng*., 2012, **3**, 445.

[2] J. B. Goodenough and K. -S. Park, *J. Am. Chem. Soc*., 2013, **135**, 1167.

[3] J. R. Dahn, T. Zheng, Y. Liu, J.S. Xue, *Science*, 1995, **270**,590.

[4] Y. S. Cohen, Y. Cohen and D. Aurbach, *J. Phys. Chem. B*, 2000, **104**, 12282.

[5] Y. Qi, H. Guo, L. G. Hector and A. Timmons, *J. Electrochem. Soc.*, 2010, **157**, A558.

[6] D. Larcher, S. Beattie, M. Morcrette, K. Edstrom, J. -C. Jumas and J. -M. Tarascon, *J. Mater. Chem*., 2007, **17**, 3759.

[7] J. Cabana, L. Monconduit, D. Larcher and M. R. Palacin, *Adv. Mater.*, 2010, **22**, E170.

[8] A. Magasinski, P. Dixon, B. Hertzberg, A. Kvit, J. Ayala and G. Yushin, *Nat. Mater.*, 2010, **9**, 353.

[9] L. -F. Cui, R. Ruffo, C. K. Chan, H. Peng and Y. Cui, *Nano Lett.*, 2009, **9**,

491.

[10] M. -H. Park, M. G. Kim, J. Joo, K. Kim, J. Kim, S. Ahn, Y. Cui and J. Cho, *Nano Lett*., 2009, **9**, 3844.

[11] M. Armand and J.-M. Tarascon, *Nature*, 2008, **451**, 652.

[12] M. S. Whittingham, *Chem. Rev.*, 2004, **104**, 4271.

[13] M. S. Whittingham, *Science*, 1976, **192**, 1126.

[14] H. Wang and H. Dai, *Chem. Soc. Rev*., 2013, **42**, 3088.

[15] Shao-Horn Y, Croguennec L, Delmas C, Nelson EC, O'Keefe MA., *Nat. Mater.*, 2003, **2**, 464.

[16] R. J. Gummow, A. de Kock and M. M. Thackeray, *Solid State Ionics*, 1994, **69**, 59.

[17] Z. Chen and J. R. Dahn, *J. Electrochem. Soc*., 2002, **149**, A1184.

[18] Y. Wang, Y. Wang, E. Hosono, K. Wang and H. Zhou, *Angew. Chem. Int. Ed*., 2008, **47**, 7461.

[19] H. Liu, Q. Cao, L. J. Fu, C. Li, Y. P. Wu and H. Q. Wu, *Electrochem. commun*., 2006, **8**, 1553.

[20] P. G. Bruce, S. A. Freunberger, L. J. Hardwick and J. M. Tarascon, *Nat. Mater.*, 2012, **11**, 19.

[21] S. Evers and L. F. Nazar, *Acc. Chem. Res.,* 2013, **46**, 1135.

[22] X. Ji and L. F. Nazar, *J. Mater. Chem.*, 2010, **20**, 9821.

[23] A. Manthiram, Y. Fu, Y.-S. Su, *Acc. Chem. Res.*, 2013, **46**, 1125.

[24] Y. Yang, G. Zheng, Y. Cui, *Chem. Soc. Rev.*, 2013, **42**, 3018.

[25] Y. X. Yin, S. Xin, Y. G. Guo and L. J. Wan, *Angew. Chem. Int. Ed.*, 2013, **52**, 13186.

[26] Y. C. Lu, Q. He and H. A. Gasteiger, *J. Phys. Chem. C*, 2014, **118**, 5733.

[27] J. Nelson, S. Misra, Y. Yang, A. Jackson, Y. Liu, H. Wang, H. Dai, J. C. Andrews, Y. Cui and M. F. Toney, *J. Am. Chem. Soc.*, 2012, **134**, 6337.

[28] S. Walus, C. Barchasz, J. F. Colin, J. F. Martin, E. Elkaim, J. C. Lepretre and F. Alloin, *Chem. Commun.*, 2013, **49**, 7899.

[29] M. Cuisinier, P.-E. Cabelguen, S. Evers, G. He, M. Kolbeck, A. Garsuch, T. Bolin, M. Balasubramanian and L. F. Nazar, *J. Phys. Chem. Lett.*, 2013, **4**,

3227.

[30] X. Ji, K. T. Lee, L. F. Nazar, *Nat. Mater.*, 2009, **8**, 500.

[31] Schuster, J.; He, G.; Mandlmeier, B.; Yim, T.; Lee, K. T.; Bein, T.; Nazar, L. F. Spherical, *Angew. Chem., Int. Ed.*, 2012, **51**, 3591.

[32] Jayaprakash, N.; Shen, J.; Moganty, S. S.; Corona, A.; Archer, L. A., *Angew. Chem., Int. Ed.*, 2011, **50**, 5904.

[33] Ji, L.; Rao, M.; Zheng, H.; Zhang, L.; Li, Y.; Duan, W.; Guo, J.; Cairns, E. J.; Zhang, Y., *J. Am. Chem. Soc.*, 2011, **133**, 18522.

[34] Li, N.; Zhang, M.; Lu, H.; Hu, Z.; Shen, C.; Chang, X.; Ji, G.; Cao, J.; Shi, Y., *Chem. Commun.*, 2012, **48**, 4106.

[35] Ji, L. W.; Rao, M. M.; Aloni, S.; Wang, L.; Cairns, E. J.; Zhang, Y. G., *Energy Environ. Sci.*, 2011, **4**, 5053.

[36] C. J. Hart, M. Cuisinier, X. Liang, D. Kundu, A. Garsuch, L. F. Nazar, *Chem. Commun.*, 2015, **51**, 2308.

[37] Q. Zhang, Y. Wang, Z. W. Seh, Z. Fu, R. Zhang, Y. Cui, *Nano Lett.*, 2015, **15**, 3780.

[38] S. Xin, L. Gu, N.-H. Zhao, Y.-X. Yin, L.-J. Zhou, Y.-G. Guo, L.-J. Wan,

J. Am. Chem. Soc., 2012, **134**, 18510.

[39] Z. Li, L. Yuan, Z. Yi, Y. Sun, Y. Liu, Y. Jiang, Y. Shen, Y. Xin, Z. Zhang, Y. Huang, *Adv. Energy Mater.*, 2014, **4**, 1301473.

[40] H. J. Peng and Q. Zhang, *Angew. Chem. In. Ed.*, 2015, **54**, 11018.

[41] X. Ji, S. Evers, R. Black, L. F. Nazar, *Nat. Commun.*, 2011, **2**, 325.

[42] J. Zheng, J. Tian, D. Wu, M. Gu, W. Xu, C. Wang, F. Gao, M. H. Engelhard, J.-G. Zhang, J. Liu, J. Xiao, *Nano Lett.*, 2014, **14**, 2345.

[43] Q. Pang, D. Kundu, M. Cuisinier, L. F. Nazar, *Nat. Commun.*, 2014, **5**, 4759.

[44] H. Yao, G. Zheng, P.-C. Hsu, D. Kong, J. J. Cha, W. Li, Z. W. Seh, M. T. McDowell, K. Yan, Z. Liang, V. K. Narasimhan, Y. Cui, *Nat. Commun.*, 2014, **5**, 3943.

[45] J. Song, M. L. Gordin, T. Xu, S. Chen, Z. Yu, H. Sohn, J. Lu, Y. Ren, Y. Duan, D. Wang, *Angew. Chem. Int. Ed.*, 2015, **54**, 4325.

[46] X. Liang, A. Garsuch, L. F. Nazar, *Angew. Chem. Int. Ed.*, 2015, **54**, 3907.

[47] J. Song, T. Xu, M. L. Gordin, P. Zhu, D. Lv, Y.-B. Jiang, Y. Chen, Y.

Duan, D. Wang, *Adv. Funct. Mater.*, 2014, **24**, 1243.

[48] G. Zhou, Y. Zhao, A. Manthiram, *Adv. Energy Mater.*, 2015, **5**, 1402263.

[49] M. Naguib, M. Kurtoglu, V. Presser, J. Lu, J. Niu, M. Heon, L. Hultman, Y. Gogotsi, M. W. Barsoum, *Adv. Mater.*, 2011, **23**, 4248.

[50] J. Q. Huang, Q. Zhang, H. J. Peng, X. Y. Liu, W. Z. Qian and F. Wei, *Energy Environ. Sci.*, 2014, **7**, 347.

[51] H. Al Salem, G. Babu, C. V. Rao and L. M. Arava, *J. Am. Chem. Soc.*, 2015, **137**, 11542.

[52] Y.-J. Li, J.-M. Fan, M.-S. Zheng and Q.-F. Dong, *Energy Environ. Sci.*, 2016, DOI: 10.1039/c6ee00104a.

[53] Y. Yang, G. Zheng, S. Misra, J. Nelson, M. F. Toney and Y. Cui, *J. Am. Chem. Soc.*, 2012, **134**, 15387.

[54] F. Wu, J. T. Lee, F. Fan, N. Nitta, H. Kim, T. Zhu and G. Yushin, *Adv. Mater.*, 2015, **27**, 5579.

[55] C. Zu, M. Klein and A. Manthiram, *J. Phys. Chem. Lett.*, 2014, **5**, 3986.

[56] K. Cai, M.-K. Song, E. J. Cairns and Y. Zhang, *Nano Lett.*, 2012, **12**,

6474.

[57] S. Meini, R. Elazari, A. Rosenman, A. Garsuch and D. Aurbach, *J. Phys. Chem. Lett.*, 2014, **5**, 915.

Chapter 2. A simple electrochemical method to improve the cycle performance of Li-S batteries

2.1. Introduction

Sulfur is one of the most promising candidates for next-generation battery cathode materials because of its high theoretical specific capacity (i.e., 1672 mAh g^{-1}). Furthermore, sulfur is very cheap and abundant on Earth. Although the lithium-sulfur (Li-S) battery has many advantages, its commercialization with liquid electrolytes has been hampered by the following issues. Firstly, the loading level of the sulfur cathode and the sulfur utilization are rather limited because of the extremely low electrical conductivity of sulfur (i.e., 5×10^{-30} S cm^{-1} at room temperature) [1]. Secondly, a series of polysulfide species produced during the charge and discharge processes are easily dissolved in organic electrolytes. Dissolved polysulfide species spontaneously diffuse out from the cathode, resulting in active material loss; they also react with the lithium metal anode, which leads to self-discharge [2,3]. Thirdly, an electrically insulating and insoluble Li_2S compound precipitates and

agglomerates on the cathode surface during prolonged cycling, which leads to the continuous increase of cell impedance; this produces an electrochemically inaccessible region, which results in the fading of the battery's capacity [4].

One of the most effective and popular methods of overcoming the problems mentioned above is based on the infiltration of sulfur into carbonaceous materials with high specific surface areas and large pore volumes (e.g., highly ordered meso- and/or micro-porous carbon) [5,6]. The high surface area not only increases the electronic contact area between carbon and sulfur, but also provides more reaction sites. Furthermore, the pores in carbonaceous materials can physically trap dissolved polysulfides and accommodate the volume change during cycling, which is beneficial for maintaining electronically conductive networks. However, the preparation of porous carbon materials involves complex and expensive processes. In addition, further heat treatment is required to allow for the infiltration of sulfur into porous carbon materials, which is a time- and energy-consuming process. Therefore, there exists a considerable impetus for developing a commercially available method to prevent rapid capacity fading.

Herein, we introduce a powerful and economical method through a very simple electrochemical control to improve the cycle life performance. Several

discharge and charge cycles at high-potential regions (i.e., above 2.2 V vs. Li/Li^+) before cycling result in the dissolution of a certain amount of polysulfide into the electrolyte, as well as the redistribution of sulfur on the cathode. Ultimately, these processes significantly enhance the cycle retention of the Li-S battery.

2.2. Experimental section

2.2.1. Materials preparation

The cathode slurry was prepared by mortar mixing 50 wt% sulfur (Sigma-Aldrich), 30 wt% conductive carbon black (Super P), and 20 wt% polyvinylidene fluoride (PVDF) polymer binder with *N*-methyl-2-pyrrolidinone as a mixing solvent. The slurry was pasted onto an aluminum current collector through the doctor blade method. After drying overnight at 60 ºC, the resulting slurry-coated aluminum foil was roll-pressed and cut into the required dimensions with a punching machine. The sulfur loading in the cathode disk was around 1 mg cm^{-2}.

To prepare the dissolved polysulfide catholyte, sublimed sulfur powder and an appropriate amount of lithium sulfide (Alfa Aesar) were added to the appropriate amount of blank electrolyte to render 0.25 M sulfur in the form of Li_2S_6 in the solution. The solution was heated at 45 ºC in an Ar-filled glove box for 18 h.

2.2.2. Characterizations and electrochemical test

Electrochemical cell tests were conducted on 2032 coin-type half cells with lithium foil as counter and reference electrode, which were fabricated in an Ar-filled glove box. The electrolyte solution was 1 M lithium bis(trifluoromethanesulfone)imide (LiTFSI) in a mixture of 1,2-dimethoxyethane (DME) and 1,3-dioxolane (DOL) at a 1:1 volume ratio with 0.1 M $LiNO_3$ as an additive.

All electrochemical measurements were made with a WBCS3000 cycler (WonATech, Korea) at room temperature. The C-rate specified in this study was based on the mass and theoretical specific capacity of sulfur (i.e., 1672 mAh g^{-1}). The cells rested for 24 h before the electrochemical test. In a regular cycling test, the cell was galvanostatically charged and discharged in the voltage window of 3.0–1.5 V. The activation cycling consisted of discharging to 2.2 V, and then charging to 3.0 V at 0.05 C. The modified activation cycling was an identical process, except for the fact that the cell was initially charged at 0.2 C to 50 mAh g^{-1}. Scanning photoelectron microscopy measurements were carried out with an 8A1 beamline of the Pohang Light Source (PLS). Electrochemical impedance spectroscopy data were obtained with a Zahner IM6 Impedance Analyzer (Zahner, Germany)

from 100 kHz to 10 mHz with an AC voltage amplitude of 5 mV at a 3.0 V voltage of the cell, with the Li metal foil as reference electrode. The data were analyzed using a model circuit derived by the ZView (Scribner Associates, Inc.).

2.3. Results and discussion

Li-S batteries exhibit two main discharge or charge potential plateaus. During the discharge reaction, sulfur is reduced to a long-chain polysulfide Li_2S_X ($4 \leq X \leq 8$) at the high-potential plateau region. As the discharge continues, the long-chain polysulfide is reduced to a short-chain polysulfide, and finally to lithium sulfide at the low-potential plateau region [7]. The sulfur utilization can be calculated from the specific capacity of the first plateau. The active material utilization of the electrode is related to the injected current density in various battery systems, and it is more pronounced in Li-S battery systems owing to the low electrical conductivity of sulfur. Figure 2.1 shows the specific capacity at the first plateau region for different current densities. The capacities at the current densities of 0.05 C-rate and 0.02 C-rate are about 20% and 25% higher, respectively, than that at the current density of 0.1 C-rate. Faradaic reactions and disproportionation reactions simultaneously occur at the first plateau [8]. The low current density provides enough time for both reaction processes, and finally leads to high sulfur utilization. Therefore, we attempt to increase the sulfur ratio that participated in the electrochemical reaction by cycling at a low C-rate at the high plateau region before normal cycling; this technique is referred to as “activation cycling” in this study.

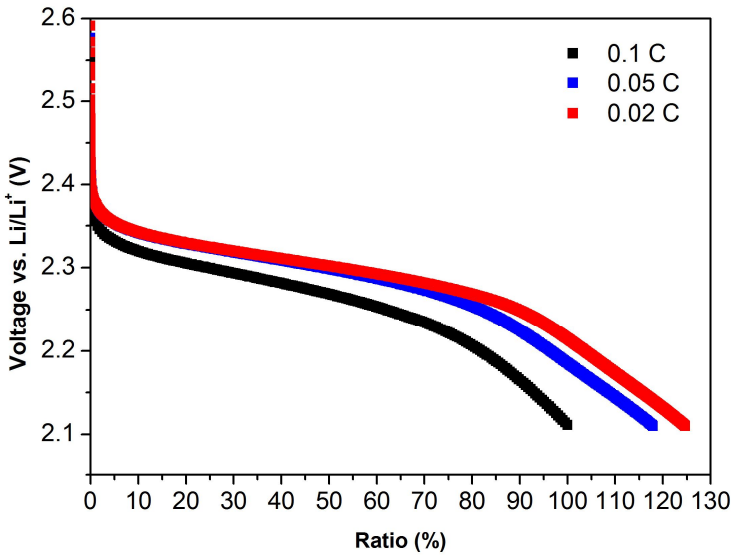

Figure 2.1. Comparison of discharge capacities at the first plateau for different C-rates.

The specific conditions for activation cycling consisted of charging and discharging at a potential window from 3.0 to 2.2 V (vs. Li/Li^+) by 0.05 C-rate. Figure 2.2 top shows the initial voltage profile with 5 cycles of activation cycling; for comparison, Figure 2.2 bottom shows the initial voltage profile without activation cycling. Interestingly, the cycle retention for the electrode with activation cycling is significantly enhanced compared to the electrode without activation cycling at 0.1 C-rate (Figure 2.3).

The irreversible capacity loss is observed in the first activation cycle (Figure 2.4) because the generated polysulfide diffuses out from the electrode during discharge, a certain portion of which cannot return to sulfur during charge. The concentration of sulfur in the electrolyte after activation cycling can be easily estimated. From Figure 2.4, an incomplete charging occurred at the first cycle. From the irreversible capacity loss, about 15% of sulfur remained in the electrolyte after the first cycle. 20 μL of the electrolyte is present in the coin cell. The complete utilization of sulfur is almost impossible [9,10]. Therefore, we can estimate the sulfur concentration to be as high as 0.23 M. In order to quantify the enhanced cycle stability for an activation-cycled cell, we prepared a 0.25 M polysulfide-dissolved electrolyte and tested the cell performance. The electrochemical properties with the polysulfide-

dissolved

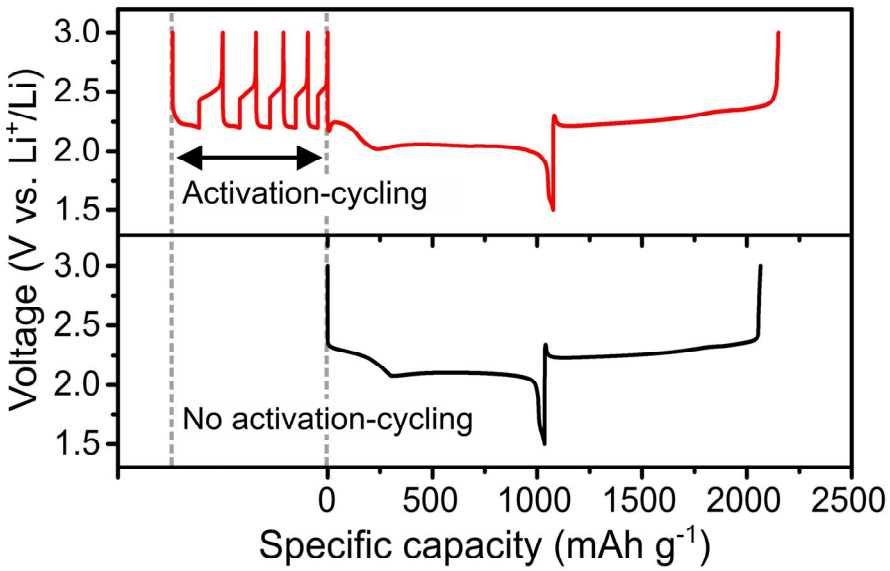

Figure 2.2. Voltage profiles at the first cycle of the sulfur cathode with activation cycling (top) and without activation cycling (bottom).

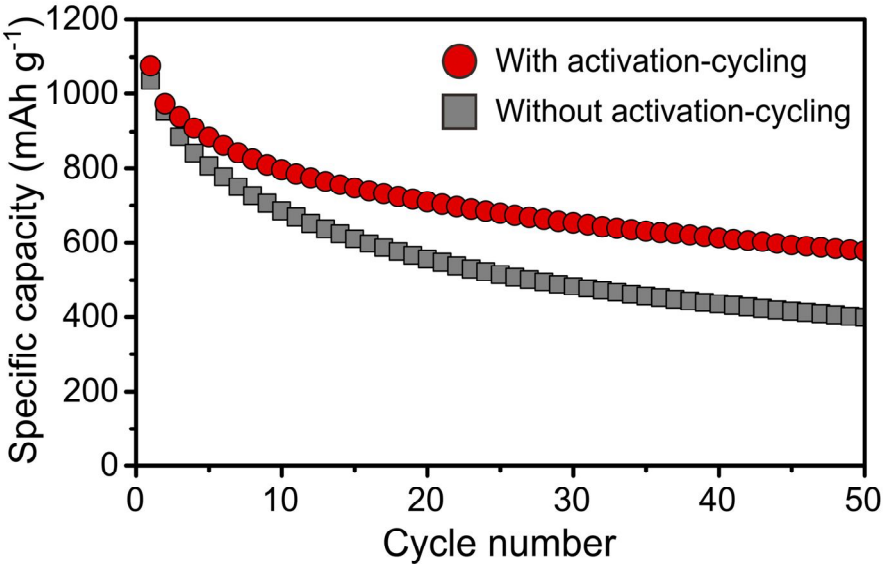

Figure 2.3. Cycle performances of the sulfur cathode with activation cycling and without activation cycling.

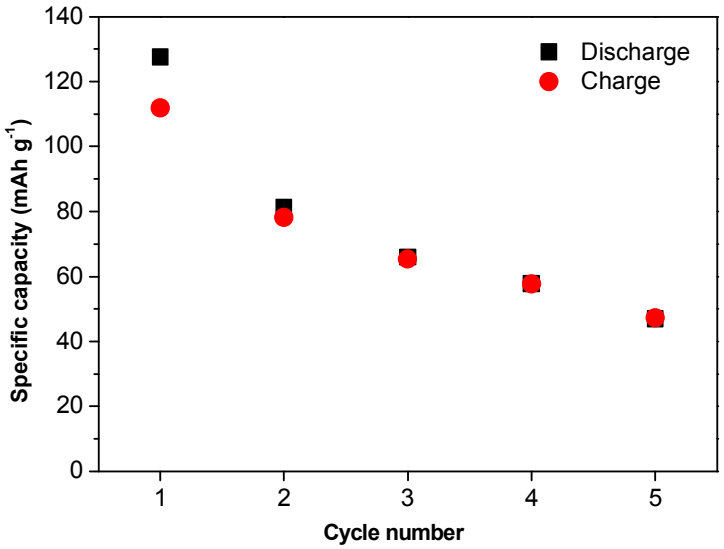

Figure 2.4. Charge and discharge specific capacities of activation-cycled cell for the initial 5 cycles.

electrolyte are very similar to those of the activation-cycled cell (Figure 2.5), which implies that the improved cycle life performance of the activation-cycled cell is closely related to the amount of dissolved polysulfide.

In fact, many research groups have reported that a certain concentration of polysulfide-dissolved electrolyte could significantly improve the cycle life performance. More specifically, the dissolved polysulfide provides a mass buffering effect, which reduces the active material dissolution during cycling [11,12]. However, in our case, the polysulfide concentration is very low, and provides a limited mass buffering effect, so it is therefore difficult to maintain that the dissolution of polysulfides is only the reason for improved cycle stability in the activation-cycled cell.

We also consider the effect of reduced charge transfer resistance by polysulfides as an additional factor. It has been reported that a small amount of polysulfide dissolved in electrolyte could act as a redox mediator, and thus effectively reduce the charge transfer resistance [13]. This phenomenon can also be supported by our experiment (see Figure 2.6). We made a Li_2S cathode by discharging a S cathode. After the first discharge cycle, the cathode was washed with the solvents 1,2-dimethoxyethane (DME) and 1,3-dioxolane (DOL) at a 1:1 volume ratio; we then reassembled the cell with fresh

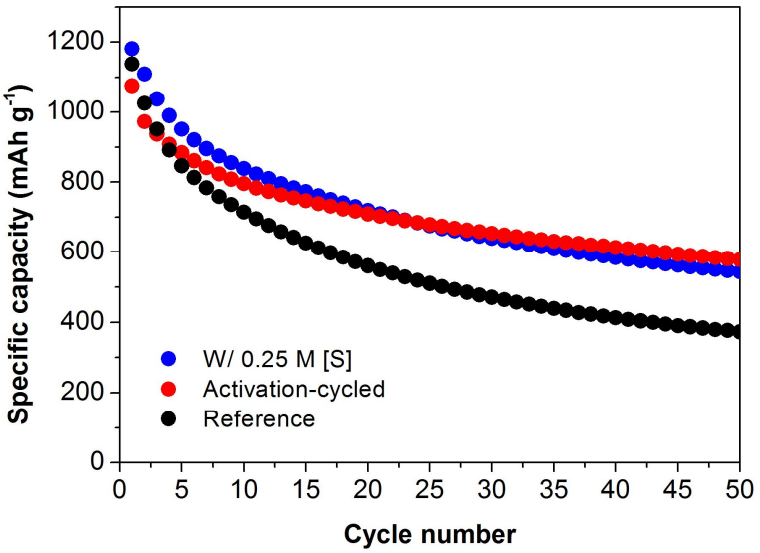

Figure 2.5. Cycle life performance of activation-cycled cells (red), cells with 0.25 M (blue), and reference cells (black) at 0.1 C.

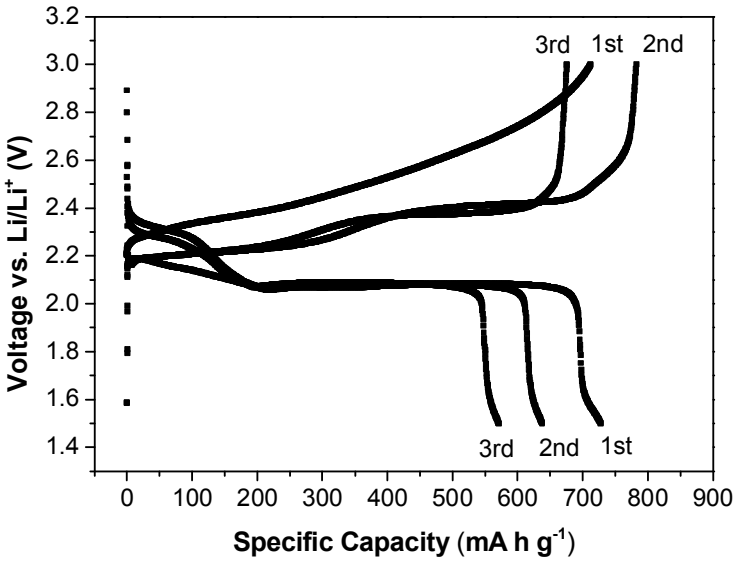

Figure 2.6. Charge and discharge profiles of a Li_2S electrode for initial three cycles (0.1 C).

electrolytes in an Ar-filled glove box. A huge overpotential was observed at the first charge, though the overpotential disappeared during following cycles. This suggests that the polysulfide dissolved in the electrolyte after the first cycle significantly decreases the charge transfer resistance.

Aside from the positive effects of polysulfide on the electrochemical properties that we mentioned above, there must be other factors that contribute to the enhancement of the cycle life of the activation-cycled cell. That is because a certain amount of polysulfide will be dissolved into the electrolyte after the first discharge for normal sulfur cells as well, and the cycle retention properties of an activation-cycled are even better than those of a cell with a 0.25 M polysulfide-dissolved electrolyte (Figure 2.7). Therefore, in order to elucidate the enhanced cycle property of activation-cycled cell, we conducted electrochemical impedance spectroscopy (EIS), and proposed a simplified equivalent circuit based on the shape of the Nyquist plots (inset of Figure 2.8). The experimental points are well described by the equivalent circuit. R1 corresponds to the resistance of the electrolyte. The semicircle is represented by a parallel circuit consisting of a resistance (R2) and a constant phase element (CPE2). The straight line in the low-frequency region is modeled by CPE1. The constant phase element (CPE) replaces the capacitor

in order to compensate for

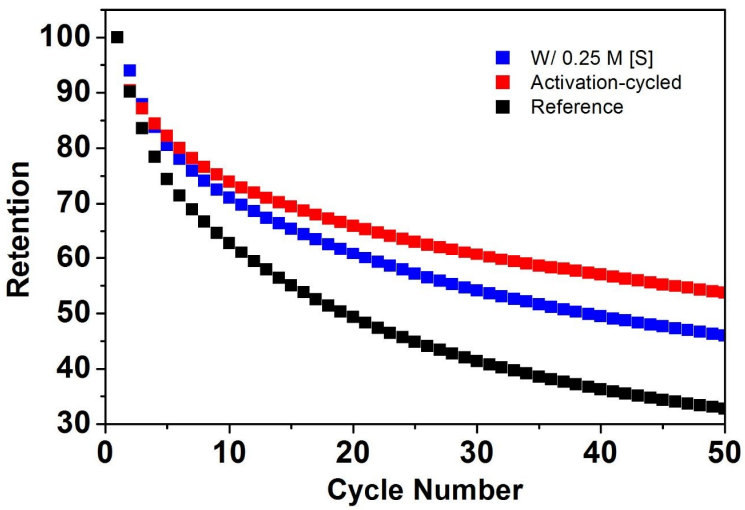

Figure 2.7. The cycle retention of cells during 50 cycles. The cycle retentions of activation-cycled cell, cell with 0.25 M, and reference cells are 53.7, 46.0, 32.7%, respectively.

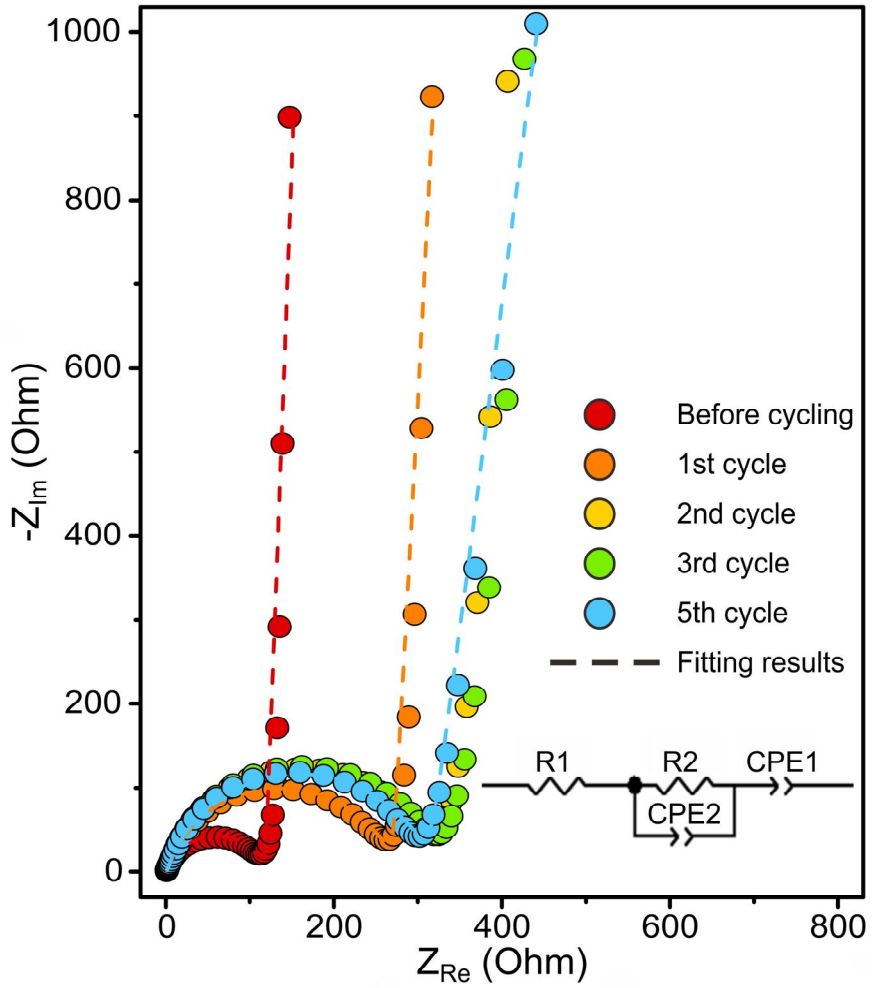

Figure 2.8. Nyquist plots of a lithium-sulfur cell during 5 activation-cycles. Inset shows the equivalent circuit applied for fitting.

Table 2.1. Resistance and capacitance values obtained from fitting results of EIS.

ACT-CYC	R1 (Ω)	R2 (Ω)	CPE2-T (F)	CPE2-P	CPE1-T (F)	CPE1-P
0	**0.77**	**118**	**2.21×10^{-5}**	**0.80**	**1.75×10^{-3}**	**0.98**
1	**0.90**	**270**	**1.27×10^{-5}**	**0.81**	**1.70×10^{-3}**	**0.97**
5	**1.26**	**312**	**0.99×10^{-5}**	**0.81**	**1.51×10^{-3}**	**0.92**

the non-ideal behavior of the electrode. CPE1-T is two orders of magnitude larger than CPE2-T, which implies that CPE1 results from a large carbon surface (Table 2.1). Moreover, it is observed that the resistance (R2) significantly increased after the activation cycles, which is attributed to the increased interphase contact resistance [14]. The insulating sulfur on surface of carbon particle could increase the interphase contact resistance, indicating that much more carbon surface is covered by sulfur after activation cycles. Furthermore, the CPE2 can be assigned to the capacitance from carbon-carbon interphase. The CPE2 can be decreased when the carbon particles detached from cathode or carbon-carbon contact insulated by sulfur. If the reason is carbon detachment, the CPE1 value, relate to the carbon electrolyte interphase, will decreased much more (like CPE2, decreased more than 50%). Therefore, we can say that sulfur redistribution in cathode structure was happened during activation-cycling.

The capacitance can be expressed by Equation 1 as follows:

$$C = \varepsilon_r \varepsilon_0 A/d \qquad (1)$$

where C is the capacitance (F), A is the area of overlap between the two plates (m^2), ε_r is the relative static permittivity (sometimes called the dielectric constant) of the material between the plates (for a vacuum, $\varepsilon_r = 1$), ε_0 is the

electric constant (ε_0 = 8.854 x 10^{-12} F m^{-1}), and d is the separation between the plates (m). For a single battery cell, the parameters are almost constant during activation cycling, except for the area A. Therefore, the capacitance is in direct proportion to the electrochemically active surface area (ECSA) of carbon. The capacitance (CPE1-T) is reduced by 14% after 5 activation cycles. This means that the ECSA of carbon decreases as a result of being covered with sulfur. Ultimately, the rearrangement of sulfur in the cathode is induced through repetitive dissolution and precipitation processes.

We modified the activation cycle conditions to further improve the dispersion of sulfur (see Figure 2.9). More specifically, polysulfides were oxidized to sulfur at the high-potential charging plateau region. The nucleation of sulfur occurs at the initial charging region, which is followed by nucleation growth. In order to make more nuclei, the charging C-rate at the nucleation region during activation cycles was increased. The large overpotential at the beginning of charging process is related to the activation energy of nucleation at 0.2 C rate. However, the overpotential becomes rather smaller compared to that in reference electrode after activation cycling (Figure 2.10). The capacitance of modified activation cycle is further reduced by 21% from EIS result (Figure 2.11). After more effective dispersion of

sulfur, the cycle life

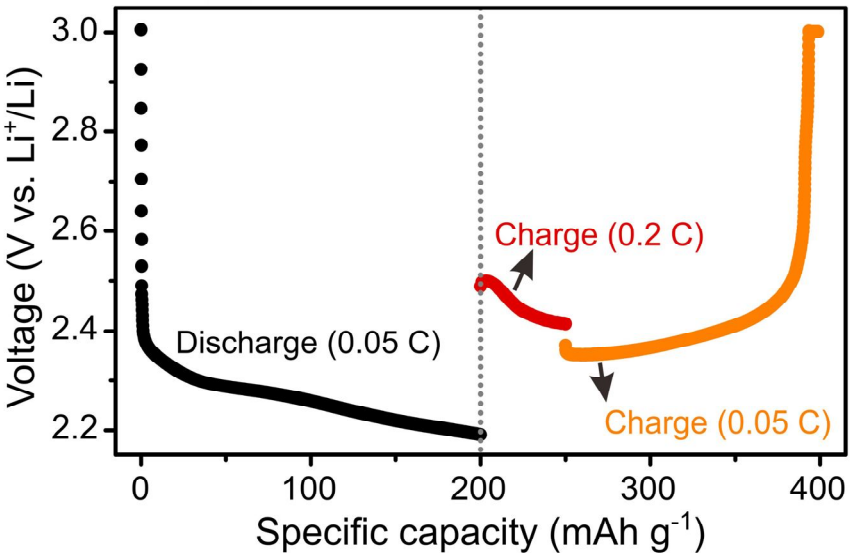

Figure 2.9. Voltage profiles of modified activation cycling.

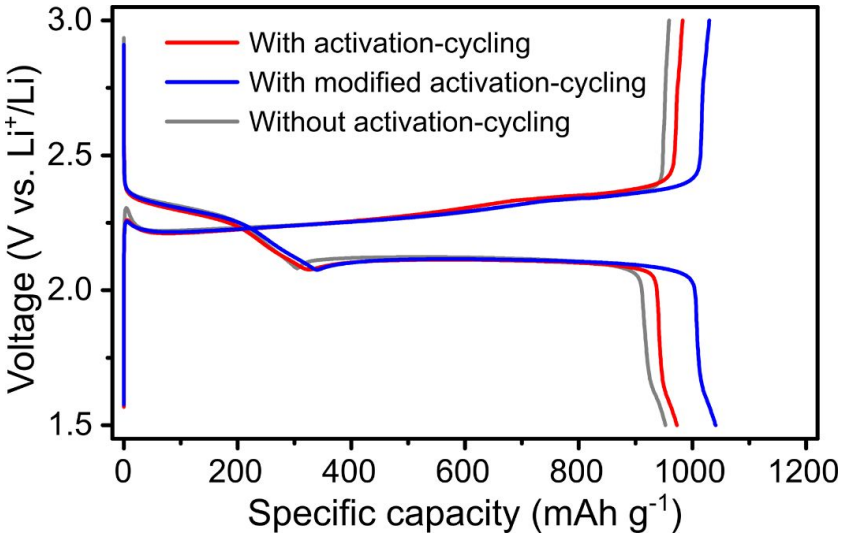

Figure 2.10. Charge and discharge curves of reference, activation-cycled and modified activation-cycled cells for the second cycle.

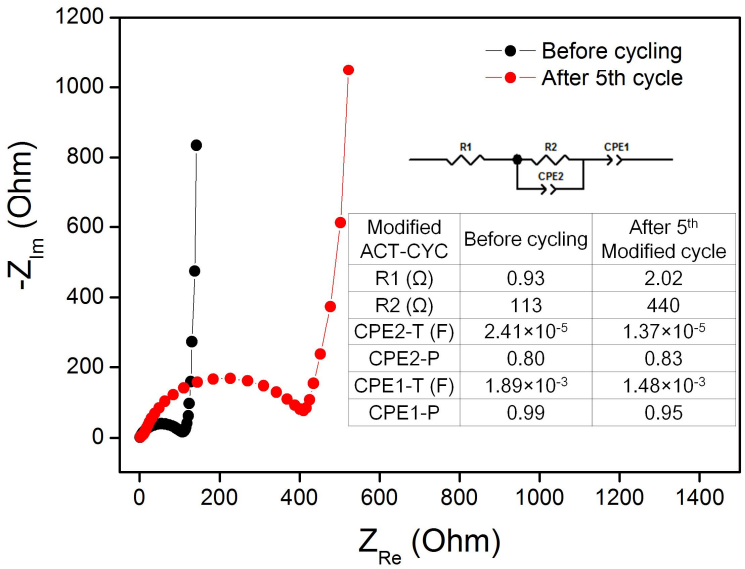

Modified ACT-CYC	Before cycling	After 5th Modified cycle
R1 (Ω)	0.93	2.02
R2 (Ω)	113	440
CPE2-T (F)	2.41×10^{-5}	1.37×10^{-5}
CPE2-P	0.80	0.83
CPE1-T (F)	1.89×10^{-3}	1.48×10^{-3}
CPE1-P	0.99	0.95

Figure 2.11. Nyquist plots of modified activation-cycles. Inset shows the fitting results of EIS.

performance of the modified activation-cycled cell is much improved (Figure 2.12). The specific capacity of the modified activation-cycled cell after 50 cycles is about twice as large as that of the cell without activation cycling. Furthermore, the capacity decay rate of the modified activation-cycled cell is only 0.7% per cycle for 50 cycles; on the other hand, the capacity of the cell without activation cycling decays at a rate of 1.4% per cycle.

In order to further understand the enhanced cycle properties of activation-cycled cells, scanning photoelectron microscopy (SPEM) analysis was performed. SPEM is a powerful tool for mapping a specific element at identical chemical state. Figure 2.13a, b, and c show SPEM images of S^0 (binding energy, 163.9 eV) before activation cycling, after activation cycling, and modified activation cycling, respectively. The images are taken from an area of 200 × 200 μm with a 1 × 1 μm resolution. Before activation cycling, there were several agglomerated sulfur clusters present (Figure 2.13a). However, after activation cycling, no agglomerated sulfur regions were observed (Figure 2.13b). In addition, the sulfur was dispersed more homogeneously after modified activation cycling (Figure 2.13c). Sulfur experiences serious phase transitions (solid-liquid-solid) during cycling. Therefore, it will induce significant stress and damage the cathode during full

discharge, which can be more pronounced at the sulfur-agglomerated regions. We effectively dispersed sulfur through activation cycling, which reduced the damage from volume change during subsequent cycling, and ultimately enhanced the cycle life.

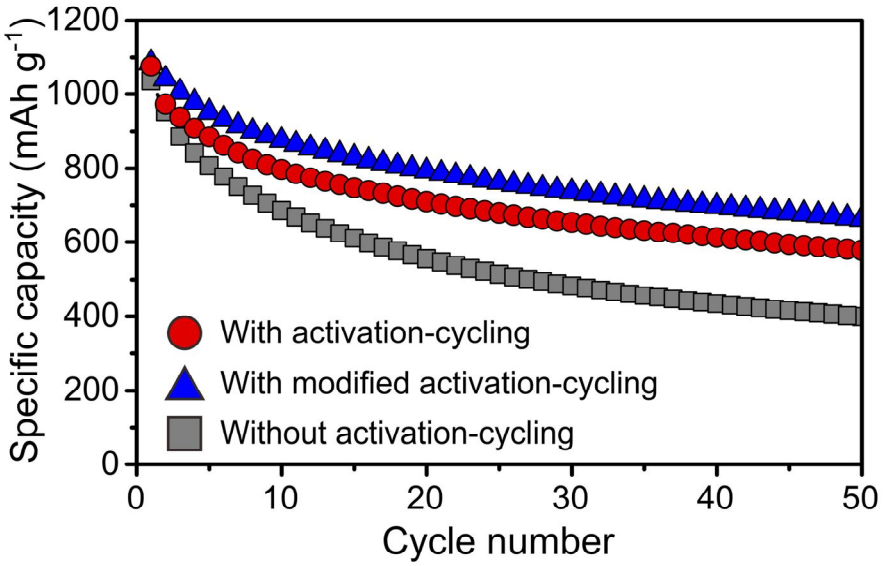

Figure 2.12. Cycle performances of sulfur cathode with modified activation cycling (0.1 C-rate).

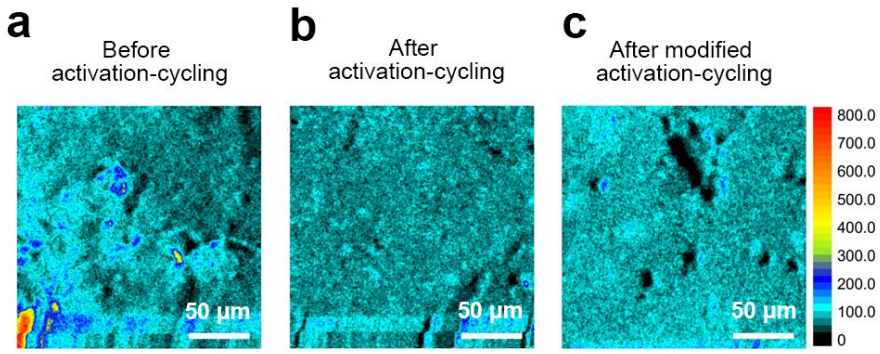

Figure 2.13. Scanning photoelectron microscopy (SPEM) mapping of (a) an as-prepared sulfur electrode, (b) a sulfur electrode after activation cycling, and (c) a sulfur electrode after modified activation cycling. The scale bars in (a-c) are 50 μm.

2.4. Conclusions

In summary, we have demonstrated a simple electrochemical method for improving the cycle life of a Li-S battery. Through precisely controlling the charging and discharging at the polysulfide dissolution region, the redistribution of sulfur at the electrode structure and the partial dissolution of polysulfide was observed (see Figure 2.14). We expect that this simple strategy can be applied to other Li-S battery systems in order to effectively limit capacity fading.

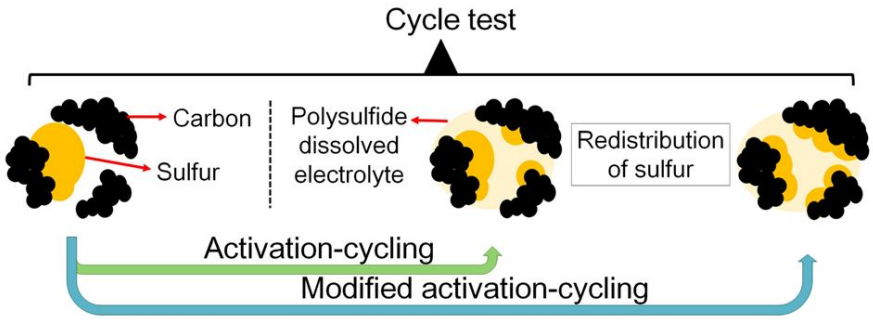

Figure 2.14. Schematic illustration of partially dissolved polysulfide and sulfur redistribution under activation cycling and modified activation cycling.

2.5. References

[1] J. A. Dean, *Lange's Handbook of Chemistry*, 3rd ed.; McGraw-Hill: New York, 1985.

[2] H. Yamin and E. Peled, *J. Power Sources*, 1983, **9**, 281.

[3] R. D. Rauh, F. S. Shuker, J. M. Marston and S. B. Brummer, *J. Inorg. Nucl. Chem.*, 1977, **39**, 1761.

[4] S.-E. Cheon, K.-S. Ko, J.-H. Cho, S.-W. Kim, E.-Y. Chin and H.-T. Kim, *J. Electrochem. Soc.*, 2003, **150**, A800.

[5] X. Ji, K. T. Lee and L. F. Nazar, *Nat. Mater.*, 2009, **8**, 500.

[6] S. Xin, L. Gu, N.-H. Zhao, Y.-X. Yin, L.-J. Zhou, Y.-G. Guo and L.-J. Wan, *J. Am. Chem. Soc.*, 2012, **134**, 18510.

[7] S. Walus, C. Barchasz, J.-F. Colin, J. F. Martin, E. Elkaim, J.-C. Lepretre and F. Alloin, *Chem. Commun.*, 2013, **49**, 7899.

[8] Y.-C. Lu, Q. He and H. A. Gasteiger, *J. Phys. Chem. C*, 2014, **118**, 5733.

[9] M. Cuisinier, P.-E. Cabelguen, S. Evers, G. He, M. Kolbeck, A. Garsuch, T. Bolin, M. Balasubramanian and L. F. Nazar, *J. Phys. Chem. Lett.*, 2013, **4**,

3227.

[10] J. Nelson, S. Misra, Y. Yang, A. Jackson, Y. Liu, H. Wang, H. Dai, J. C. Andrews, Y. Cui and M. F. Toney, *J. Am. Chem. Soc.*, 2012, **134**, 6337.

[11] S. S. Zhang and J. A. Read, *J. Power Sources*, 2012, **200**, 77.

[12] S. Chen, F. Dai, M. L. Gordin and D. Wang, *RSC Adv.*, 2013, **3**, 3540.

[13] Y. Yang, G. Zheng, S. Misra, J. Nelson, M. F. Toney and Y. Cui, *J. Am. Chem. Soc.*, 2012, **134**, 15387.

[14] Z. Deng, Z. Zhang, Y. Lai, J. Liu, J. Li and Y. Liu, *J. Electrochem. Soc.*, 2013, **160**, A553.

Chapter 3. Discharging a Li-S battery with ultra-high sulfur content cathode using a redox mediator

3.1. Introduction

Li-S batteries have attracted much recent attention, due to the low cost and high theoretical specific capacity (1672 mAh g^{-1}) of sulfur [1,2]. They have great potential as energy storage devices for electric vehicles (EVs) and energy storage systems (ESSs) [3]. However, there are several obstacles for their commercialization. One is the presence of polysulfides, which are intermediate products formed during charge/discharge, and their dissolution into the electrolyte leads to continuous loss of the active material and self-discharge [4,5]. Past researches have focused on constraining the movement of polysulfides by infiltrating sulfur into meso and/or micro porous carbon materials, physically restricting the dissolution of polysulfides [6-9], or designing a surface (e.g., functionalized carbon, metal oxide or metal carbide) that effectively adsorbs polysulfides [10-14]. Another major obstacle is the insulating nature of sulfur. In order to compensate for the low electrical

conductivity of sulfur (5×10^{-30} S cm^{-1} at room temperature), 30-40 wt% conductive agent is typically needed. This also necessitates the use of a binder (10-20 wt%) to attach the conductive agent and active material onto the current collector. The conductive agent and binder limited the amount of sulfur in the cathode to 50-60 wt% [6,7,11,12], leading to significantly lowered energy density and specific capacity per cathode mass, as well as increased manufacturing cost. The solution is increasing the effective conductivity of the cathode at high sulfur loading. To the best of our knowledge, all studies reporting high sulfur mass loading in Li-S batteries have achieved it by using thick cathodes [15-18]. This increases the areal capacity but not the volumetric capacity, even though the latter is more meaningful criterion [19]. Improving the volumetric capacity requires a higher sulfur ratio in the cathode material. Infiltrating sulfur into porous carbon only provides a limited solution, since the increased sulfur ratio is achieved at the cost of reduced conductivity from carbon. Additional conductive agents are needed in these composites, therefore sulfur loading in the cathodes remains low [20].

In this paper, the effective cathode conductivity is increased by introducing a redox mediator cobaltocene into the electrolyte. It has a redox

potential within the region of polysulfide reduction, and therefore can act as an electron transfer agent between the conductive surface and polysulfides. We will show that cobaltocene enabled Li_2S nucleation and growth not only on the conductive carbon surface but also in the electrolyte. This redox mediator allows us to achieve significant improvement in the electrochemical performance of the cathode with ultra-high sulfur content (80 wt%).

3.2. Experimental section

3.2.1. Materials preparation

The blank electrolyte consists of 1 M lithium bis (trifluoromethanesulfone) imide (LiTFSI) in a mixture of 1,2-dimethoxyethane (DME) and 1,3-dioxolane (DOL) at a 1:1 volume ratio, with 0.1 M $LiNO_3$ as an additive. To prepare the polysulfide catholyte, sulfur powder (Alfa Aesar) and lithium sulfide (Alfa Aesar) in fixed ratio were added to the blank electrolyte to achieve 1 M sulfur concentration in the form of Li_2S_6. The catholyte was heated at 45 ^{0}C for 24 h. A designated amount of cobaltocene was prepared at room temperature after stirring for 12 h. All processes were performed in an Ar-filled glove box.

Sulfur loaded commercial carbon non-woven layer (GDL, Toray) was prepared by dropping sulfur dissolved CS_2 solution onto GDL electrode. After drying at 60 ^{0}C, the sulfur loading mass was controlled from 1.2 to 1.3 mg cm^{-2}.

The 80 wt% sulfur cathode slurry was created by mixing sulfur, carbon (Super P and multi-walled carbon nanotube (MWCNT) in 1:1 mass ratio) and polyvinylidene difluoride (PVDF) binder with N-Methyl-2-pyrrolidone (NMP)

solvent in weight percentages of 80%, 10% and 10%, respectively. The slurry was pasted onto an Al current collector through the doctor blade method, and dried at 60 ^{0}C for 12 h. The coated foil was then roll-pressed and cut into 11 mm-diameter disks with a punching machine. The sulfur loading mass was 1.3-1.5 mg cm^{-2}. The same procedure was used to prepare the 70 wt% sulfur cathode, except that slurry was made of 70 wt% sulfur, 15 wt% carbon (Super P and MWCNT in 2:1 mass ratio) and 15 wt% PVDF binder. The 50 wt% sulfur cathode was prepared from a 5:3:2 mixture of S, Super P and PVDF.

3.2.2. Characterizations and electrochemical test

The volumetric capacity was calculated based on cathode volume (except Al foil). The thickness of cathode was measured using Micrometer measurement.

The 2032 coin-type half cells were assembled using the sulfur cathode and catholyte from above. The counter and reference electrodes were fabricated from lithium foil in an Ar-filled glove box. All electrochemical measurements were carried out using a WBCS3000 cycler (WonATech, Korea) at room temperature. The cyclic voltammogram (CV) tests were performed at a sweep rate 0.2 mV s^{-1}. The C-rates used in this study were based on the mass and theoretical specific capacity of sulfur (i.e., 1672 mAh g^{-1}).

X-ray absorption near-edge fine structure (XANES) was measured at 8C nano-probe XAFS beamline (BL8C) of Pohang Light Source (PLS-II) in the 3.0 GeV storage ring with a ring current of 360 mA. The radiation source of BL8C is a tapered in-vacuum-undulator. The X-ray beam was monochromated by a Si(111) double crystal and then it was delivered to a secondary source aperture where the beam size was adjusted to be 0.3 mm (v) × 1 mm (h). A high voltage (3000 V) was applied to ionization chambers which were filled with N_2/Ar mixture gases to detect x-ray intensity. XAFS measurement was conducted in a transmission mode. The samples were

prepared with solvent wetted glass fiber separators. After wetting, the glass fibers were covered with Kapton tape. The obtained spectra were processed using Demeter software. In order to align the spectra Co foil was measured simultaneously with the samples.

The in-situ XRD analysis was carried out at 5D beamline of the Pohang Light Source. The in-situ cells were assembled with specially prepared 2032 coin cells. The coin cells had a Kapton tape window in the center. The morphology and structure of products were characterized with a field-emission scanning electron microscope (FESEM, ZEISS, MERLIN Compact).

3.3. Results and discussion

To measure the redox potentials of sulfur, cyclic voltammogram (CV) test was performed using a sulfur-loaded commercial carbon non-woven layer (gas diffusion layer, GDL) as the working electrode, and Li metal as the counter electrode. In Figure 3.1a, two pairs of electrochemical redox peaks appear. The high potential reduction peak (2.30 V vs. Li/Li^+) involves the reduction of sulfur into long-chain polysulfides (Li_2S_X, $4 \leq X \leq 8$). The low potential reduction peak (2.05 V) indicates the reduction of polysulfides to Li_2S. Note that the area under the 2.05 V reduction peak is smaller than that of the 2.30 V peak, it is opposite from typical behavior in Li-S batteries [21-23]. The reason will be discussed later. A separate CV test was performed in a coin cell with 50 mM cobaltocene dissolved electrolyte, using a bare GDL as working electrode. From Figure 3.1b, cobaltocene has a sharp redox potential at 2.00 V, which is lower than the second reduction peak of sulfur (2.05 V). Therefore, in principle, cobaltocene has the potential capability for reducing polysulfides to Li_2S.

In order to test this possibility, we prepared three coin cells with different concentration of cobaltocene (0 mM, 12.5 mM and 25 mM) in 1 M [S] catholyte in Li_2S_6 form. The working and counter electrodes were GDL and Li

metal, respectively. All tests were performed under galvanostatic discharge conditions

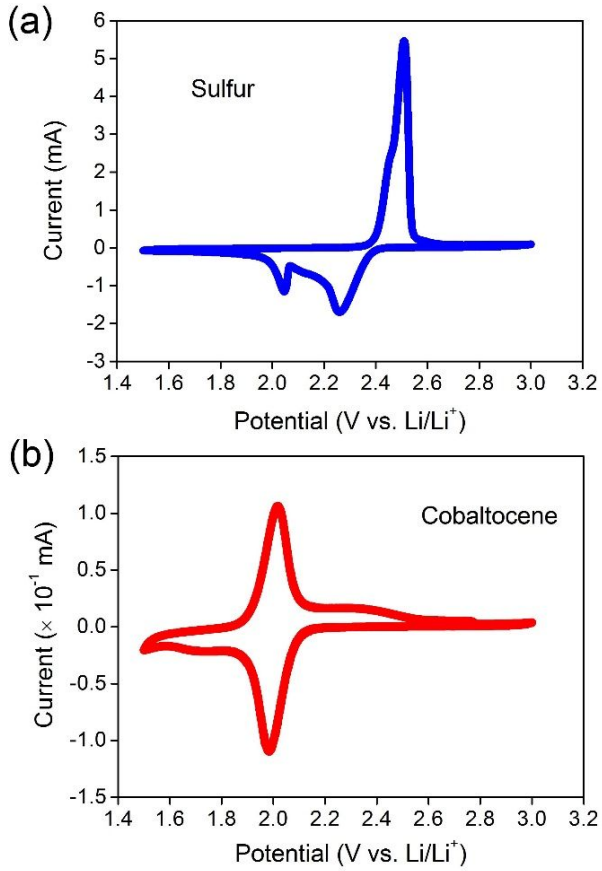

Figure 3.1. (a) Cyclic voltammograms of sulfur and (b) cobaltocene. The sweep rate was 0.2 mV s^{-1}.

with a current density of 500 μA cm^{-2}. Sinxe the active material was a polysulfide, there is no high discharge plateau (at about 2.30 V) related to the reduction of sulfur to polysulfides [24], as shown in Figure 3.2. The discharge capacity increases with cobaltocene concentration. According to the CV results, 50 mM cobaltocene only contributes 30 μAh cm^{-2} to the discharge capacity. Therefore, the increased capacity here is not from cobaltocene itself, but from the low discharge plateau where the polysulfides are reduced to Li_2S.

Scanning electron microscope (SEM) images of bare GDL and after the first discharge (Figures 3.3a–d) show a large number of highly agglomerated Li_2S particles when the concentration of cobaltocene is increased. It is a clear evidence that cobaltocene effectively reduces the polysulfides to solid Li_2S. Typical Li-S batteries have a potential plateau at 2.1–2.0 V after a gently sloping region between 2.3–2.1 V. However, this plateau almost disappeared in the absence of cobaltocene. This can be understood from the magnified SEM images. The surface of bare carbon fiber was clear and smooth (Figure 3.4a), but completely covered with Li_2S particles (Figure 3.4b) after discharge. Since Li_2S is insoluble in the electrolyte and has high electrical resistivity, electron transfer from conductive carbon surface to the Li_2S/electrolyte interface incurs high polarization [25]. More specifically, the limited

conductive surface area

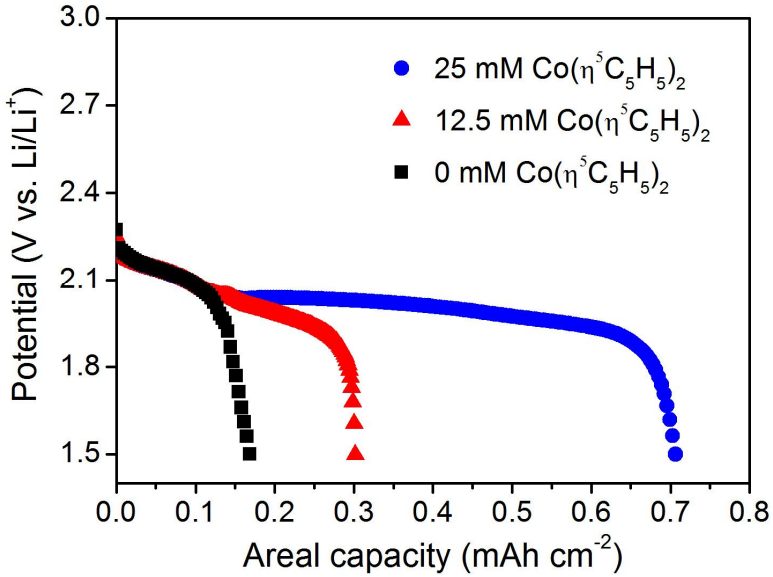

Figure 3.2. Galvanostatic discharge curves of cells with different concentrations (0, 12.5, 25 mM) of cobaltocene in 1 M [S] catholyte.

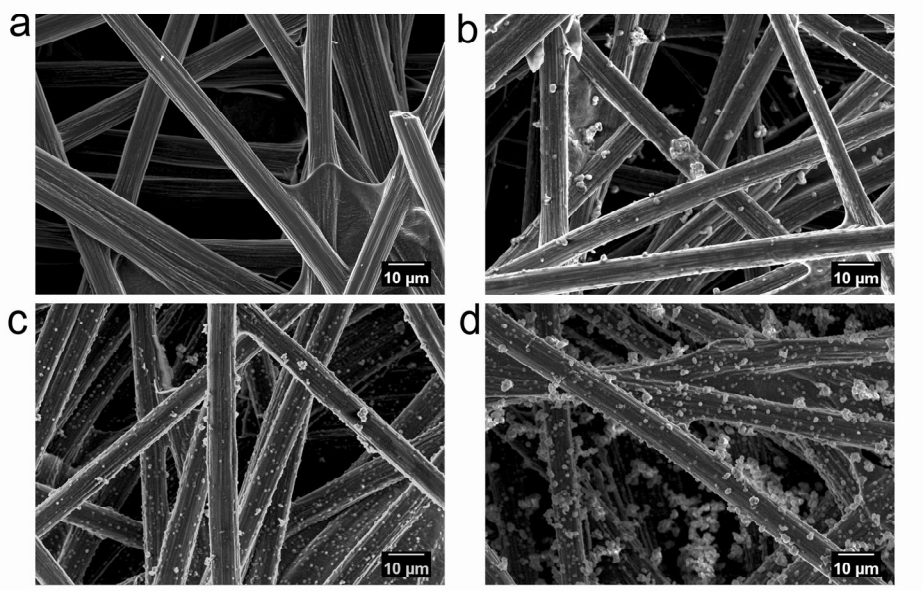

Figure 3.3. SEM images of (a) bare GDL and after discharge with (b) 0 mM, (c) 12.5 mM, and (d) 25 mM cobaltocene.

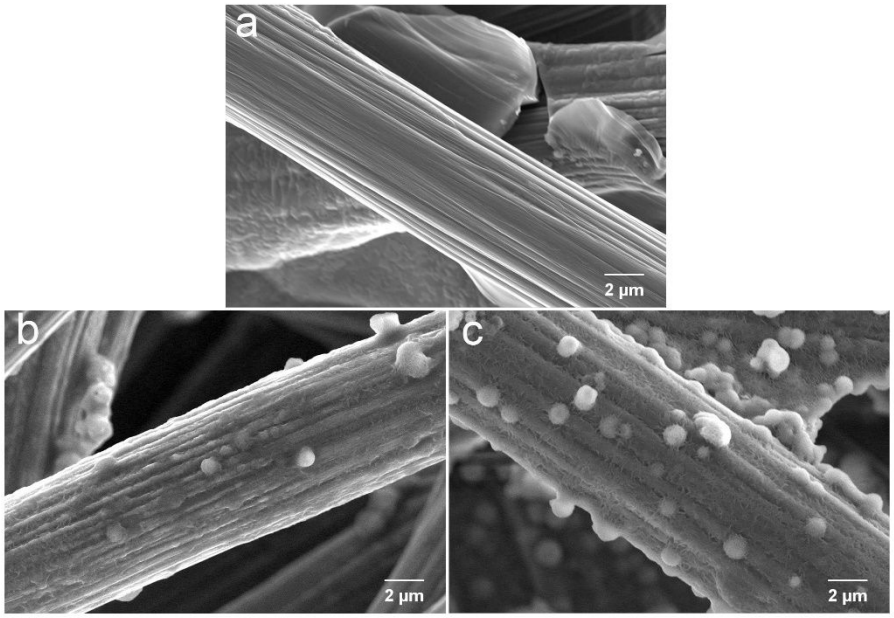

Figure3.4. Magnified SEM images of bare (a) GDL, after discharge with (b) 0 mM, (c) 25 mM cobaltocene in catholyte.

cannot support enough sites to accommodate Li_2S, leading to the characteristic potential drop and limited discharge capacity. The redox mediator acts as an electron transfer agent between conductive surface and polysulfides: it is reduced directly at the carbon fiber surface to M^{red}, which diffuses into the electrolyte, then reduce the polysulfides there while itself is oxidized back to M^{ox}. Hence the redox mediator allows Li_2S nucleation and growth on the carbon surface and in the electrolyte simultaneously. Afterwards, Li_2S nanoparticles in the electrolyte will attach to and agglomerate with those already on the carbon surface to reduce the surface energy (Figure 3.5). As a result, cobaltocene in the electrolyte allows not only more Li_2S formation but also a thicker Li_2S layer (Figure 3.4c). We also quantitatively demonstrated it using energy-dispersive X-ray spectroscopy (EDS) analysis (Figure 3.6). It also showed the same results that large amount of sulfur species was formed with increased concentration of redox mediator.

In order to confirm that the cobaltocene (M^{red}) reduces polysulfides by being oxidized into cobaltocenium (M^{ox}), we conduct X-ray absorption near-edge structure (XANES) analysis. Figure 3.7 shows the normalized Co K-edge XANES spectra for M^{red} (0.5 M cobaltocene in electrolyte) and M^{ox} (obtained by adding polysulfides into M^{red} and stirring for 6 h) at energies

corresponding

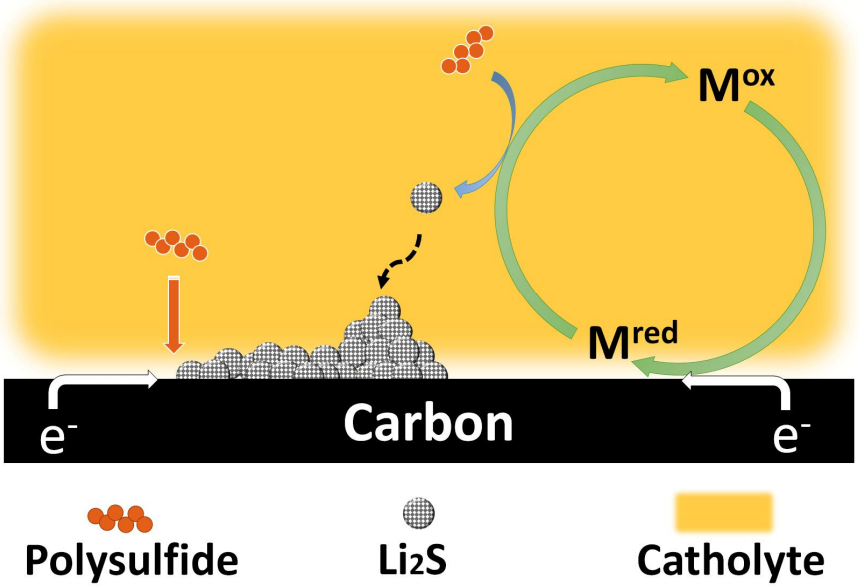

Figure 3.5. Schematic illustration of unified mechanism. Li_2S nucleation and growth through conductive surface pathway and solution pathway with cobaltocene.

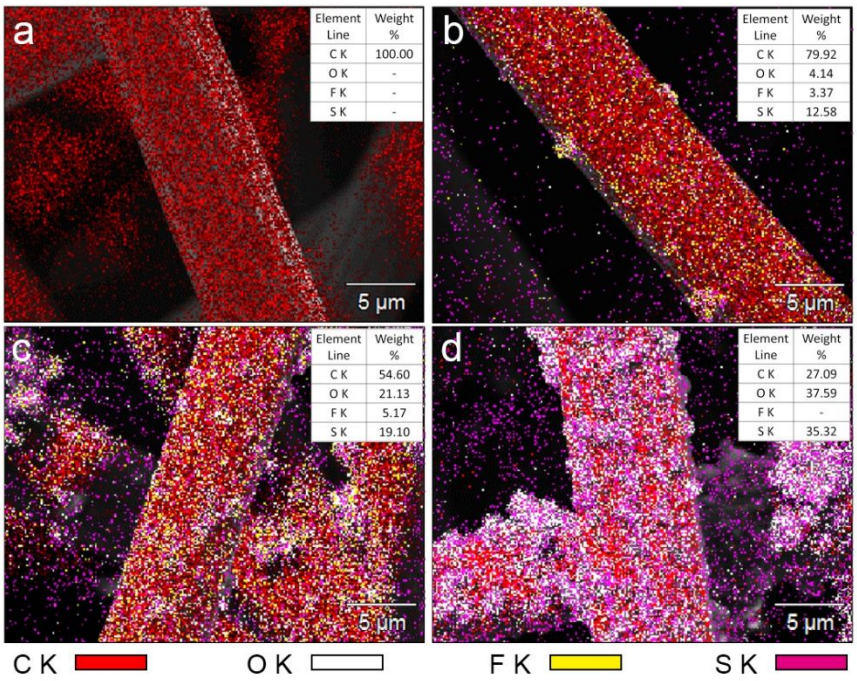

Figure 3.6. EDS elemental mapping of (a) bare GDL, after discharge with (b) 0 mM, (c) 12.5 mM, (d) 25 mM cobaltocene. The inset shows the quantitative results.

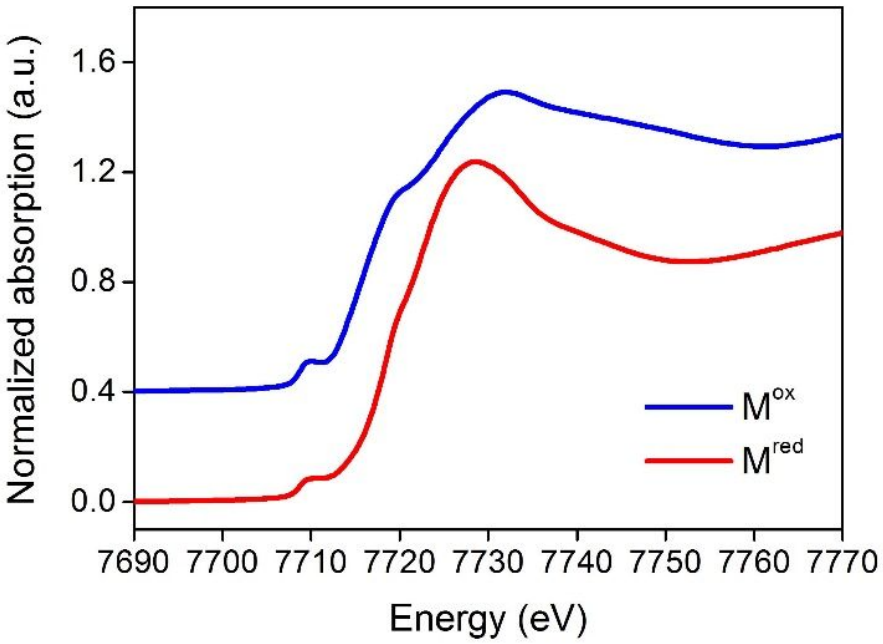

Figure 3.7. Normalized Co K-edge XANES spectra for M^{red} and M^{ox}.

to the electronic transition from Co 1s to 4p. There are three peaks in the rising edge region. The pre-edge peak at 7710 eV corresponds to electric dipole-forbidden (1s → 3d) transition, which is enabled by 4p-3d hybridization due to the distortion of local structure. The absorption peak at 7720 eV is assigned to 1s → Cp (π*) transition (Cp is cyclopentadienyl). The strong peak at the top of the edge is 1s → 4p transition (7730 eV) [26-29]. As the reaction proceeds, the 1s → 4p transition energy (above 7720 eV) increases and the peak shifts from 7728 to 7732 eV, presenting clear evidence of the oxidation of Co^{2+} (cobaltocene) into Co^{3+} state (cobaltocenium). In addition, the intensities of pre-edge peak and the shoulder on the rising edge are increased. Similar results have been reported for other organometallic compounds (e.g., ferrocenium, the oxidized state of ferrocene) [30].

To further verify that the increased capacity is from Li_2S formation, we conducted in-situ X-ray diffraction (XRD) analysis during the first cycle with and without 50 mM cobaltocene. A cathode with 70 wt% S, 15 wt% carbon and 15 wt% binder was used as the working electrode. The cells were galvanostatic charged/discharged at 200 μA cm^{-2}. Without cobaltocene, the intensities of orthorhombic α-sulfur (PDF no. 00-008-0247) peaks gradually decreased during the initial discharge and completely disappeared after the

high potential region (Figure 3.8). No additional identical peak was found until the end of the discharge. It suggests that there is no detectable crystalline Li_2S. Nevertheless, the gradually sloping (as opposed to a plateau) discharge curve at the low potential region is due to a thin insulating Li_2S layer covering the conductive carbon surface and hindering charge transfer. As explained earlier, this layer leads to limited discharge capacity from the low potential plateau. With cobaltocene, in contrast, there is a clear discharge potential plateau for Li_2S formation. XRD patterns also display Li_2S (111) Bragg peak at 19.5 nm^{-1} (PDF no. 00-023-0369) towards the end of discharge (Figure 3.9). It could be interpreted that more and larger Li_2S particles were formed in the presence of cobaltocene. The complete disappearance of the Li_2S peak during the charging process means that the thick Li_2S layer formed through solution and surface reactions is effectively converted to polysulfides and then to sulfur. The Li_2S particles in direct contact with the conductive surface can be easily charged. However, their insulating nature inhibits the charging of Li_2S particles away from the conductive surface. Cui's group reported polysulfides could act as a redox mediator during the charging process [31]. Our group also reported similar result recently [32]. A small amount of polysulfides in electrolyte could effectively reduce the charging overpotential. This is also the

case here. The

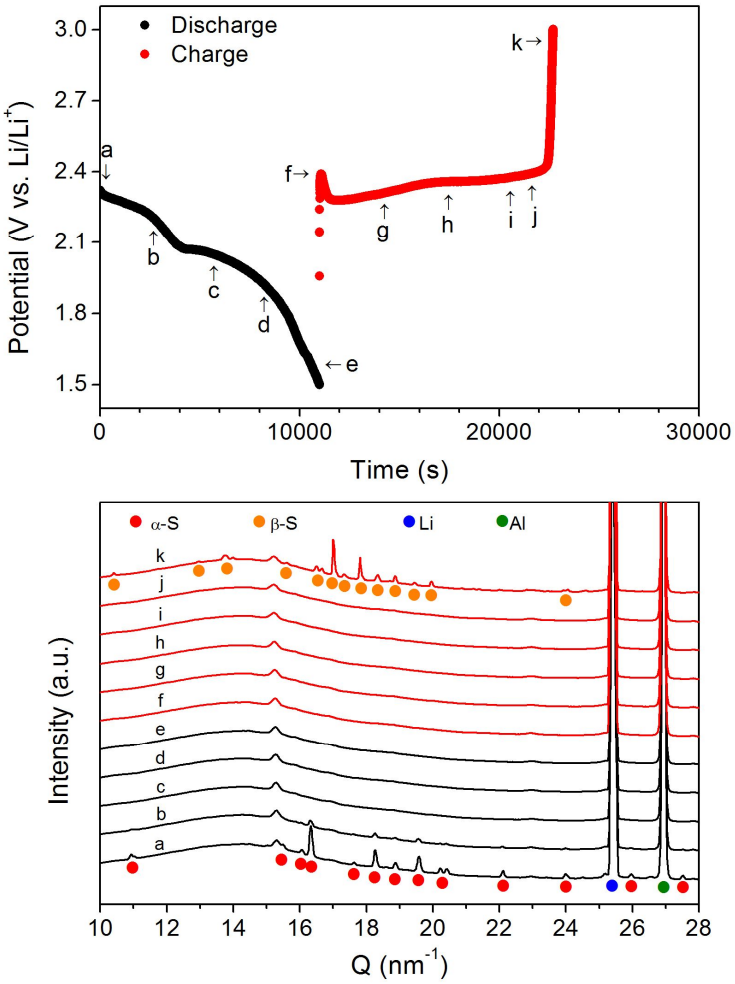

Figure 3.8. Galvanostatic discharge-charge curves of first cycle and corresponding in-situ XRD patterns for points labeled on the curves without cobaltocene.

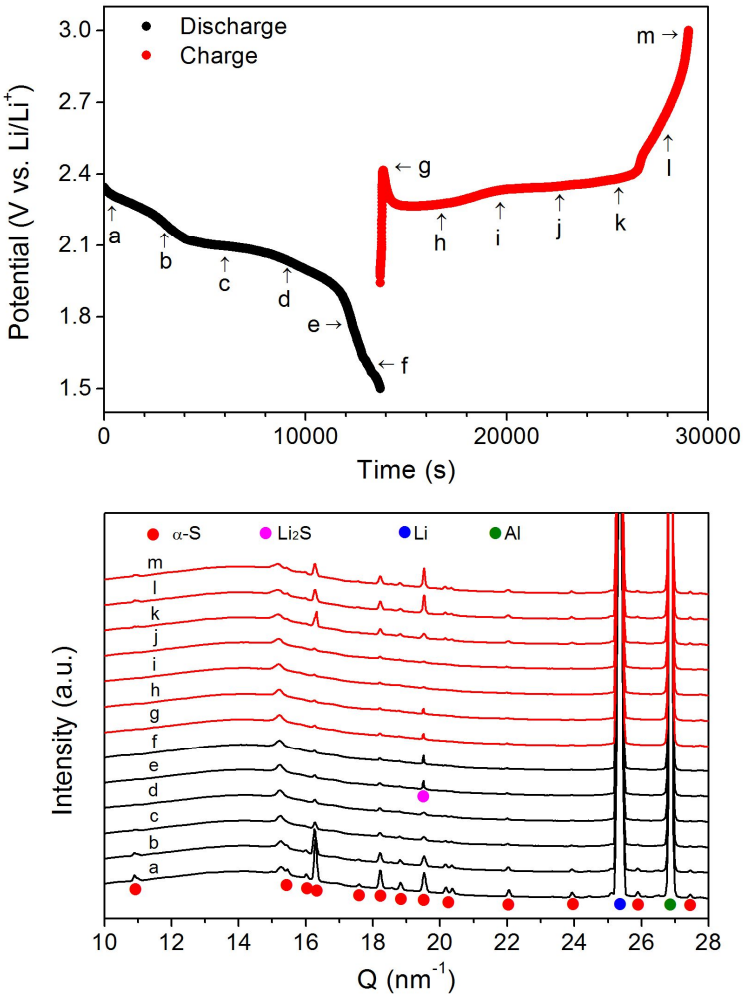

Figure 3.9. Galvanostatic discharge-charge curves of first cycle and corresponding in-situ XRD patterns for points labeled on the curves with 50 mM cobaltocene.

long chain polysulfides migrate to Li_2S and produce short chain polysulfides through disproportionation reaction. The short chain polysulfides could dissolve into the electrolyte and participate in the charging process.

The results discussed so far show that cobaltocene can transfer electrons from electrode to the polysulfieds. This could compensate for the limited conductivity of the cathode with extremely low conductive agent ratio. A cathode with 80 wt% sulfur, 10 wt% carbon and 10 wt% binder was prepared by simple mortar mixing method. When cells using this cathode were cycled at 0.1 C (167.2 mA g^{-1}_S) with and without 50 mM cobaltocene, the initial discharge capacities were dramatically different, as seen in Figure 3.10. After several cycles, the cell with cobaltocene displayed a capacity of about 750 mAh g^{-1}_S, while the reference cell delivered only 200 mAh g^{-1}_S, which is mainly from the high potential plateau region (Figure 3.11). As explained earlier, the low capacity without cobaltocene is due to the limited amount of conductive carbon, which not only transfers electrons but also provides sites for Li_2S nucleation and growth. The redox mediator cobaltocene acts as a liquid conductive agent. It effectively transfers electrons from the cathode to the polysulfides, and therefore allows Li_2S nucleation and growth on and off the conductive framework.

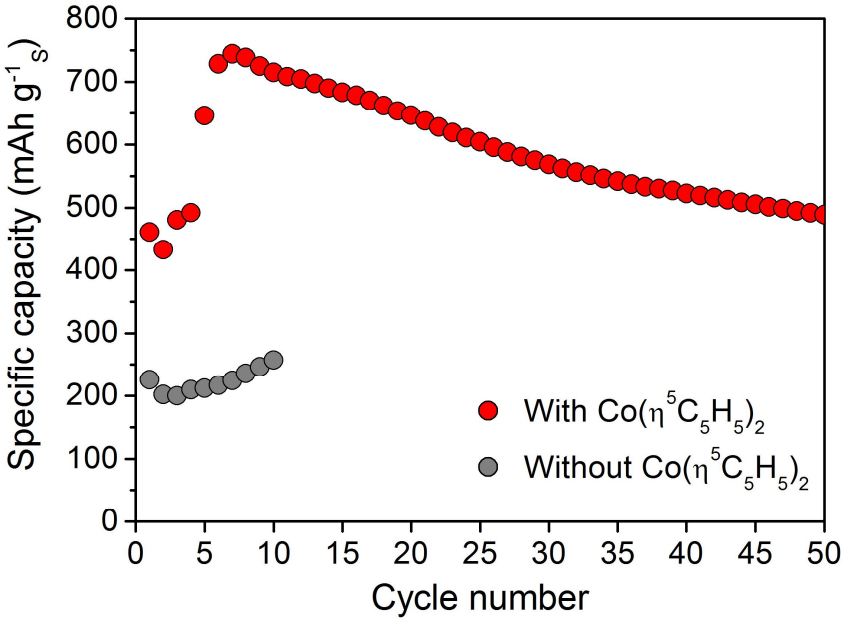

Figure 3.10. Electrochemical characterization of ultra-high sulfur content (80 wt%) cathode with and without cobaltocene. The cycle performance shows dramatically improved discharge capacity with cobaltocene.

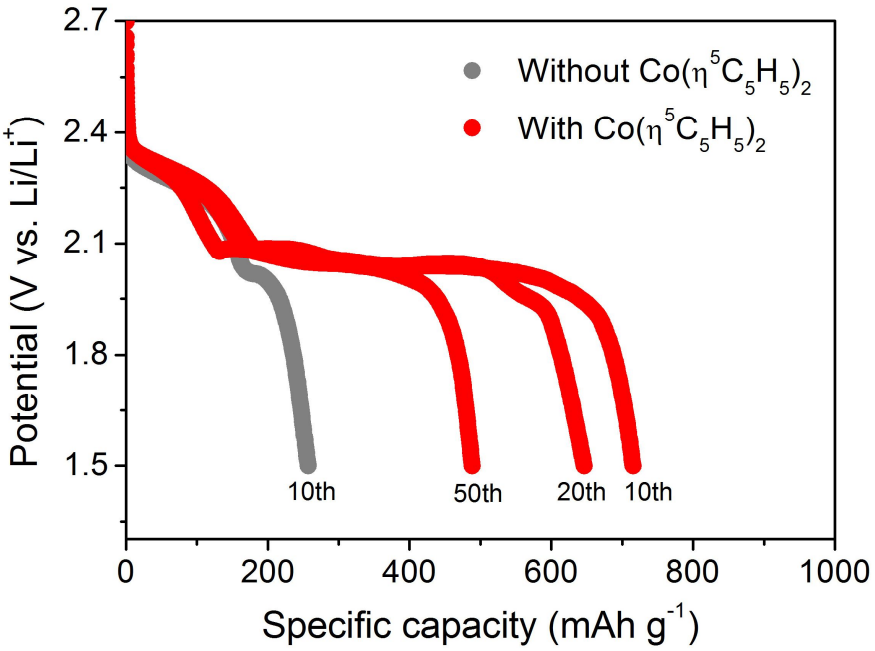

Figure 3.11. The glavanostatic discharge curves of various cycles.

Currently, the typical cathode in Li-S batteries contains only 50 wt% sulfur. Therefore, although its specific capacity based on the sulfur mass is high, the value based on total cathode mass is very low. The measured value of 200 mAh g^{-1} per cathode mass after 50 cycles (Figure 3.12) is similar to that of commercial $LiCoO_2$ cathode.[1] Our cathode with 80 wt% sulfur using cobaltocene shows 200% increased capacity after 50 cycles, which is equivalent to 800 mAh g^{-1}_S in a 50 wt% sulfur cathode. We also shown the discharge capacity based on cathode volume at Figure 3.13. The volumetric capacity is dramatically improved due to the increased sulfur content in cathode.

The rate capability performance with cobaltocene is shown in Figure 3.14. The results are only mediocre due to the ultra-high sulfur content and extremely low carbon content. The thick layer of large Li_2S particles on the conducive surface after discharge significantly hinders the following charging process. Even though the polysulfides could act as a redox mediator as described earlier, they are far less effective than cobaltocene, especially at high current density. Still, the cell was functional and delivered about 200 mAh g^{-1}_S capacity at a high current density of 1.2 A g^{-1}_S. When the charging current was fixed to 0.2 A g^{-1}_S from the 6^{th} cycle on (slow charging), the rate

capability improved remarkably. It delivers about 350 mAh g^{-1}_S capacity at 1.2 A g^{-1}_S current density. Therefore, we believe that the rate capability could be further improved with another redox mediator that could effectively recharge Li_2S.

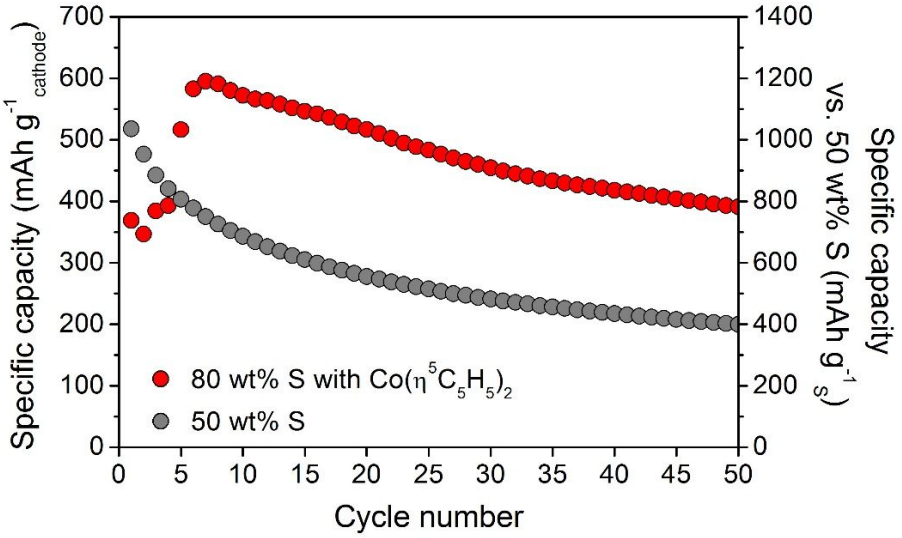

Figure 3.12. Specific capacities based on cathode mass versus cycle number. Charge/discharge current density is 0.1 C.

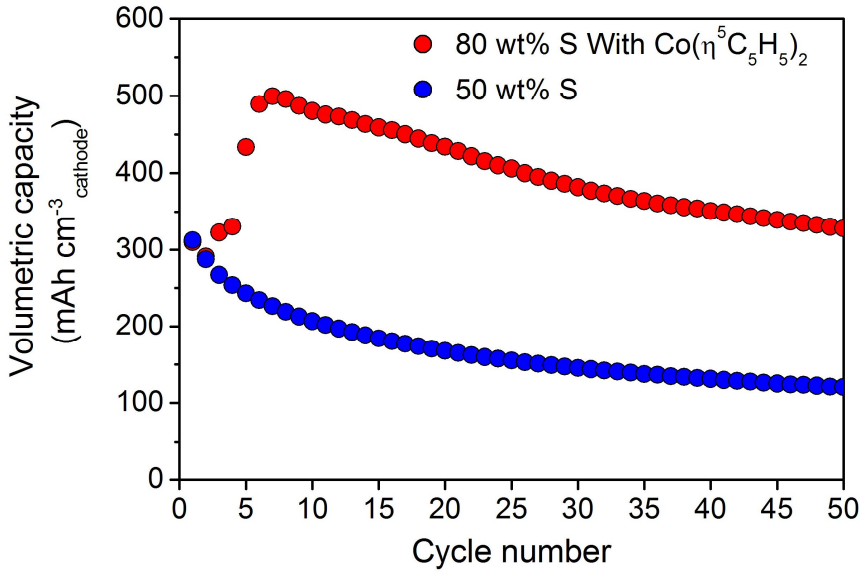

Figure 3.13. Volumetric capacities versus cycle number of 80 wt% S cathode with cobaltocene and 50 wt% S cathode. All tests were performed at 0.1 C.

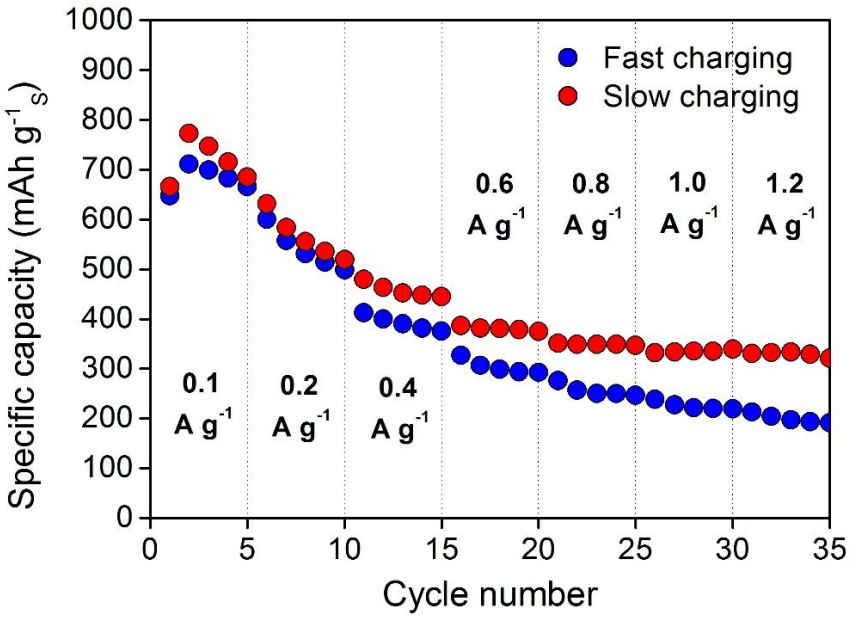

Figure 3.14. Rate performances of the cells with different charging current density. The cell is charged/discharged at indicated current density (Fast charging). The other cell is charged at 0.2 A g^{-1} from 6th cycle (Slow charging).

3.4. Conclusions

In summary, we have successfully realized the high performance Li-S battery for ultra-high sulfur content (80 wt%) cathode by using cobaltocene as a redox mediator in the electrolyte. The redox mediator acts as an electron transfer agent: it is reduced at the cathode and then oxidized by the polysulfides remote from the conductive surface to produce Li_2S. This novel approach can effectively produce Li_2S both on the conducting surface and the solution. Taken together, this unified mechanism allows sufficient Li_2S formation with a very low amount of conductive agent in the cathode, as confirmed by our electrochemical method, SEM, XANES and in-situ XRD studies. The results reported here provide a simple and scalable approach to one of the most important challenges in creating ultra-high sulfur content cathodes for Li-S batteries.

3.5. References

[1] Ji, X.; Nazar, L. F. *J. Mater. Chem.,* 2010, **20**, 9821.

[2] Marom, R.; Amalraj, S. F.; Leifer, N.; Jacob, D.; Aurbach, D. *J. Mater. Chem.,* 2011, **21**, 9938.R

[3] Bruce, P. G.; Freunberger, S. A.; Hardwick, L. J.; Tarascon, J.-M. *Nat. Mater.,* 2011, **11**, 19.

[4] Lu, Y.-C.; He, Q.; Gasteiger, H. A. *J. Phys. Chem. C,* 2014, **118**, 5733.

[5] Rauh, R. D.; Shuker, F. S.; Marston, J. M.; Brummer, S. B. *J. Inorg. Nucl. Chem.,* 1977, **39**, 1761.

[6] Ji, X.; Lee, K. T.; Nazar, L. F. *Nat. Mater.,* 2009, **8**, 500.

[7] Xin, S.; Gu, L.; Zhao, N.-H.; Yin, Y.-X.; Zhou, L.-J.; Guo, Y.-G.; Wan, L.-J. *J. Am. Chem. Soc.,* 2012, **134**, 18510.

[8] Li, Z.; Jiang, Y.; Yuan, L.; Yi, Z.; Wu, C.; Liu, Y.; Strasser, P.; Huang, Y. *ACS Nano,* 2014, **8**, 9295.

[9] Li, Z.; Yuan, L.; Yi, Z.; Sun, Y.; Liu, Y.; Jiang, Y.; Shen, Y.; Xin, Y.; Zhang, Z.; Huang, Y. *Adv. Energy Mater.,* 2014, **4**, 1301473.

[10] Wang, H.; Yang, Y.; Liang, Y.; Robinson, J. T.; Li, Y.; Jackson, A.; Cui, Y.; Dai, H. *Nano Lett.,* 2011, **11**, 2644.

[11] Liang, X.; Hart, C.; Pang, Q.; Garsuch, A.; Weiss, T.; Nazar, L. F. *Nat. Commun.,* 2015, **6**, 5682.

[12] Tao, X.; Wang, J.; Ying, Z.; Cai, Q.; Zheng, G.; Gan, Y.; Huang, H.; Xia, Y.; Liang, C.; Zhang, W.; Cui, Y. *Nano Lett.,* 2014, **14**, 5288.

[13] Hart, C. J.; Cuisinier, M.; Liang, X.; Kundu, D.; Garsuch, A.; Nazar, L. F. *Chem. Commun.,* 2015, **51**, 2308.

[14] Liang, X.; Garsuch, A.; Nazar, L. F. *Angew. Chem. Int. Ed.,* 2015, **54**, 3907.

[15] Qie, L.; Manthiram, A. *Adv. Mater.,* 2015, **27**, 1694.

[16] Song, J.; Xu, T.; Gordin, M. L.; Zhu, P.; Lv, D.; Jiang, Y.-B.; Chen, Y.; Duan, Y.; Wang, D. *Adv. Funct. Mater.,* 2014, **24**, 1243.

[17] Lv, D.; Zheng, J.; Li, Q.; Xie, X.; Ferrara, S.; Nie, Z.; Mehdi, L. B.; Browning, N. D.; Zhang, J.-G.; Graff, G. L.; Liu, J.; Xiao, J. *Adv. Energy Mater.,* 2015, **5**, 1402290.

[18] Li, D.; Han, F.; Wang, S.; Cheng, F.; Sun, Q.; Li, W.-C. *ACS Appl. Mater. Interfaces,* 2013, **5**, 2208.

[19] Obrovac, M. N.; Chevrier, V. L. *Chem. Rev.,* 2014, **114**, 11444.

[20] Xu, G.-L.; Xu, Y.-F.; Fang, J.-C.; Peng, X.-X.; Fu, F.; Huang, L.; Li, J.-T.; Sun, S.-G. *ACS Appl. Mater. Interfaces,* 2013, **5**, 10782.

[21] Shim, J.; Striebel, K. A.; Cairns, E. J. *J. Electrochem. Soc.,* 2002, **149**, A1321.

[22] Jayaprakash, N.; Shen, J.; Moganty, S. S.; Corona, A.; Archer, L. A. *Angew. Chem., Int. Ed.,* 2011, **50**, 5904.

[23] Huang, J.-Q.; Zhang, Q.; Peng, H.-J.; Liu, X.-Y.; Qian, W.-Z.; Wei, F. *Energy Environ. Sci.,* 2014, **7**, 347.

[24] Zhang, S. S.; Read, J. A. *J. Power Sources,* 2012, **200**, 77.

[25] Fan, F. Y.; Carter, W. C.; Chiang, Y.-M. *Adv. Mater.,* 2015, **27**, 5203.

[26] Ignatov, A. Y.; Losovyj, Y. B.; Carlson, L.; Lagraffe, D.; Brand, J. I.; Dowben, P. A. *J. Appl. Phys.,* 2007, **102**, 083520.

[27] Lacy, D. C.; Park, Y. J.; Ziller, J. W.; Yano, J.; Borovik, A. S. *J. Am.*

Chem. Soc., 2012, **134**, 17526.

[28] Iwai, K.; Iwai, M.; Suto, K.; Nakashima, S.; Motoyama, I.; Sano, H.; Ikemoto, I.; Kosugi, N.; Kuroda, H. *Bull. Chem. Soc. Jpn.,* 1986, **59**, 2675.

[29] Balasubramanian, M.; Giacomini, M. T.; Lee, H. S.; McBreen, J.; Sukamto, J. H. *J. Electrochem. Soc.,* 2002, **149**, D137.

[30] Atkins, A. J.; Bauer, M.; Jacob, C. R. *Phys. Chem. Chem. Phys.,* 2013, **15**, 8095.

[31] Yang, Y.; Zheng, G.; Misra, S.; Nelson, J.; Toney, M. F.; Cui, Y. *J. Am. Chem. Soc.,* 2012, **134**, 15387.

[32] Kim, K. R.; Yu, S.-H.; Sung, Y.-E. *Chem. Commun.,* 2016, **52**, 1198.

국문초록

리튬-황 전기의 성능향상을 위한 간단하고 경제적인 방법

리튬 이온 전지는 지난 수 십년간 널리 핸드폰와 노트북 등과 같은 휴대용 전자기기의 주요 동력원으로 사용되어 왔다. 현재 주로 상용되고 있는 이차 전지의 전극 소재로는 흑연 및 흑연계 탄소가 음극으로, 리튬 코발트 옥사이드가 ($LiCoO_2$) 양극으로 쓰이고 있다. 그러나 오늘날에는 전기 자동차와 대용량 에너지 저장 시스템과 같은 기존과 다른 분야에서 이차 전지에 대한 수요가 급증하고 있다. 하지만 기존의 소재들은 용량적 측면에서 더 이상 발전하기 어려운 한계에 도달했으며, 새로운 분야에 적용하기에는 가격이 비싸고 에너지 밀도가 낮다는 단점이 있다. 따라서 기존의 이차 전지 소재보다 더 큰 에너지 밀도를 가지면서 값 싼 전극 소재에 대한 연구가 활발하게 진행되고 있다.

그 중에서 황은 매우 큰 이론 용량과 (1672 mAh g^{-1}) 값 싼 가격을 가지고 있으면서 지구상에 널리 분포되어 있기 때문에 차기 양극 물질로 큰 관심을 받고 있다. 하지만 상용화 되기에는 아

직도 많은 문제점을 가지고 있다. 첫째는 황이 매우 낮은 전기 전도도와 이온 전도도를 가지고 있다는 것 이다. 이로 인하여 황의 전기화학반응에 대한 활용율이 낮고, 전극 물질로 사용할 때 많은 양의 도전제가 필요하게 된다. 따라서 양극에서 활물질인 황이 차지하는 비율이 낮아지게 되고 전극의 에너지 밀도가 떨어지게 된다. 두번째는 리튬-황 전지의 나쁜 충방전 특성이다. 그 원인은 여러가지 있지만 그 중에서 반응 중간 생성물인 polysulfides 가 지속적으로 전해질에 녹아 들어가는 점과 충방전 후에 나타나는 활물질의 부피 변화에 따른 전극 구조의 붕괴가 주된 요인으로 지적 받고 있다.

이러한 문제점들을 해결하기 위하여 다양한 시도가 보고되고 있다. 그 중에서 가장 효과적이고 많이 사용된 방법은 기공 구조가 발달되고 표면적이 큰 카본 물질 속에 황을 가두는 전략이다. 이런 전략은 황과 카본의 접촉면적을 증가하는 동시에 물리적으로 polysulfides 를 카본 구조 속에서 빠져 나가지 못하게 할 수 있다. 동시에 반응과정에서 생기는 부피 변화를 효과적으로 수용할 수 있기 때문에 전극 구조의 붕괴를 막을 수 있게 된다. 또 다른 방법은 polysulfides 를 화학적으로 결합할 수 있는 표면을 (e.g., functionalized carbon, metal oxide, metal sulfide or metal

carbide) 만들어 화학적인 흡착으로 활물질을 전극구조내에 가두는 것이다. 이런 방법들은 매우 효과적이지만 실제로 상용화 하기에는 가격이 비싸고 공정이 어려우면서 대량 생산하기가 어렵다는 단점이 있다. 따라서 이 연구에서는 경제적이고 간단한 방법으로 리튬-황 전지의 성능을 향상할 수 있는 방법들을 소개하고 있다.

먼저, 1장에서는 간단히 리튬 이온 전지 및 리튬-황 전지에 대하여 소개한다. 특히 지금 상용화 되여 있는 양극과 음극 물질에 대해서 간단히 소개하였다. 그리고 이번 연구의 중점인 리튬-황 전지에 대해서 소개하였고 현재 직면한 문제점과 그 해법에 대해서 설명 하였고, 마지막에 이번 연구의 목적에 대해서 간략하게 요약하였다.

2장에서는 간단한 전기화학적 방법을 이용하여 손쉽게 리튬-황 전지의 충방전 특성을 향상시킨 연구에 대하여 다룬다. 황이 polysufides 로 환원되는 전위 범위에서 몇번의 충전과 방전을 하게 되면 일정한 양의 polysulfides 가 전해질 속에 녹아 들어가고, 더욱이 황이 양극 구조 내에서의 재분배가 발생하게 되는 것을 알게 되었다. 결과적으로 이런 영향으로 리튬-황 전지의 충방전 특성이 현저하게 개선되게 되는데 이런 충방전 테스트 전의 과정을 여기에서는 “활성화 충방전” 이라고 명명하였다. 이런 방법은 매우

간편하고 경제적이라는 장점이 있고, 물질 디자인 없이 기본 양극 물질로 이루어진 전극의 충방전 특성을 효과적으로 향상하였다는 데 큰 의미를 가지고 있다. 이런 “활성화 충방전” 의 작동 기질을 규명하기 위하여 다양한 전기화학적 분석법과 (electrochemical impedance spectroscopy) 분광 분석법으로 (scanning photoelectron microscopy) 해석하였다.

3장에서는 산화 환원 반응 매개체를 (redox mediator) 이용하여 전극과 활물질 사이에서 전자와 홀의 운반체로 작용하여 황의 비율이 높은 (80 wt%)전극에서 부족한 전극 전도도를 효과적으로 향상하여 뛰어난 충방전 특성을 보이는 연구에 대해서 소개한다. 전해질에 용해할 수 있고 또 산화 환원 반응 전위가 polysulfides 를 환원할 수 있는 구간에 위치하는 매개체를 전해질에 용해 시켜 전극의 전도도를 효과적으로 향상 하였다. 방전시 산화 환원 반응 매개체는 양극에서 환원되는데, 이런 환원 상태의 매개체가 전해질 속의 polysulfides 와 만나면 산화되면서 polysulfides 를 환원시킨다. 이런 작동 기작을 통하여 전자는 전극에서 polysulfides 로 이동하게 된다. 다양한 전기화학적 분석법으로 산화 환원 매개체가 실제로 효과적으로 전극과 활물질 사이에서 전자와 홀을 이동시키는 것을 확인 했고, 실시간 X선 회절

분석법으로 (in-situ XRD) polysulfides 가 Li_2S 로 환원됨을 확인 했다. 나아가서 전자현미경 (scanning electron microscope), XANES (X-ray absorption near edge structure) 분석법으로 해당 반응 메커니즘을 해석하고 분석하였다.

주요어: 리튬-황 전지, 전기화학적 방법, 황의 재분배, 산화 환원 반응 매개체, 코발토신, 높은 황 비율, 경제적이고 간단한 방법

학 번: 2011-22914